

**Best Available
Copy
for all Pictures**

AD-784 952

ROTATIONAL RELAXATION MEASUREMENTS
AND RESONANT PHENOMENA IN LASER-
EXCITED HYDROGEN FLUORIDE

G. H. Lindquist, et al

Environmental Research Institute of
Michigan

Prepared for:

Army Missile Command
Advanced Research Projects Agency

June 1974

DISTRIBUTED BY:

NTIS

National Technical Information Service
U. S. DEPARTMENT OF COMMERCE
5285 Port Royal Road, Springfield Va. 22151

NOTICES

Sponsorship. The work reported herein was conducted by the Environmental Research Institute of Michigan (formerly the Willow Run Laboratories of The University of Michigan) for the Advanced Research Projects Agency of the Department of Defense and was monitored by the U.S. Army Missile Command under Contract Number DAAH01-73-C-0591, ARPA Order No. 1180. The Project Manager is Dr. F. A. Haak and the ARPA Program Manager is Dr. P. O. Clark.

Disclaimer. The views and conclusions contained in this document are those of the authors and should not be interpreted as necessarily representing the official policies, either expressed or implied, of the Advanced Research Projects Agency or of the U.S. Government.

Distribution. Initial distribution is indicated at the end of this document.

DDC Availability. Qualified requesters may obtain copies of this document from:

**Defense Documentation Center
Cameron Station
Alexandria, Virginia 22314**

Final Disposition. After this document has served its purpose, it may be destroyed. Please do not return it to the Environmental Research Institute of Michigan.

The image shows a document page with a large, handwritten letter 'A' in the bottom left corner. The document contains faint, mostly illegible text and a large, dark, diagonal mark or smudge in the upper right quadrant.

2a

UNCLASSIFIED

SECURITY CLASSIFICATION OF THIS PAGE (When Data Entered)

REPORT DOCUMENTATION PAGE		READ INSTRUCTIONS BEFORE COMPLETING FORM
1. REPORT NUMBER 101300-18-F	2. GOVT ACCESSION NO.	3. RECIPIENT'S CATALOG NUMBER AD-784952
4. TITLE (and Subtitle) ROTATIONAL RELAXATION MEASUREMENTS AND RESONANT PHENOMENA IN LASER-EXCITED HYDROGEN FLUORIDE		5. TYPE OF REPORT & PERIOD COVERED Final Report, 1 March 1973 through 28 May 1974
7. AUTHOR(s) G. H. Lindquist, L. M. Peterson and C. B. Arnold Phone (313) 483-0500		6. PERFORMING ORG. REPORT NUMBER 101300-18-F
9. PERFORMING ORGANIZATION NAME AND ADDRESS Environmental Research Institute of Michigan Infrared and Optics Division, P.O. Box 618 Ann Arbor, MI 48107		8. CONTRACT OR GRANT NUMBER (s) DAAH01-73-C-0591 ARPA Order Nr. 1180
11. CONTROLLING OFFICE NAME AND ADDRESS Advanced Research Projects Agency 1400 Wilson Blvd. Arlington, VA 22209		10. PROGRAM ELEMENT, PROJECT, TASK AREA & WORK UNIT NUMBERS
14. MONITORING AGENCY NAME AND ADDRESS (if different from Controlling Office) U.S. Army Missile Command Attn: AMSMI-RNS/Dr. F. A. Haak Redstone Arsenal, AL 35809		12. REPORT DATE June 1974
		13. NUMBER OF PAGES 55
		15. SECURITY CLASS (of this report) Unclassified
16. DISTRIBUTION STATEMENT (of this Report) Initial distribution is indicated at the end of this document.		15a. DECLASSIFICATION/DOWNGRADING SCHEDULE
17. DISTRIBUTION STATEMENT (of the abstract entered in Block 20, if different from Report)		
18. SUPPLEMENTARY NOTES Amount of contract, \$99,285; performance period, 1 March 1973 through 28 May 1974; principal investigator, George H. Lindquist		
19. KEY WORDS (Continue on reverse side if necessary and identify by block number) Hydrogen fluoride Laser absorption Optical nutation HF laser Probe laser Self-induced transparency Rotational relaxation Saturation spectroscopy Laser linewidth Laser stimulation Double resonance		
20. ABSTRACT (Continue on reverse side if necessary and identify by block number) Rates for the transfer of rotational energy (R-R) in vibrationally excited HF gas were measured using a single laser pump-probe technique. The relaxation time was found to be inversely proportional to HF pressure in the mTorr range and the self- relaxation rate constant was determined to be $k_{\text{HF-HF}} = (7.8 \pm 0.2) \times 10^7 \text{ sec}^{-1}$ Torr^{-1} for the $P_1(5)$ laser transition. (continued)		

DD FORM 1 JAN 73 1473 EDITION OF 1 NOV 65 IS OBSOLETE

UNCLASSIFIED

SECURITY CLASSIFICATION OF THIS PAGE (When Data Entered)

UNCLASSIFIED

SECURITY CLASSIFICATION OF THIS PAGE (When Data Entered)

(20. Abstract)

Rotational relaxation of HF gas due to the presence of additive gases was observed. The relaxation rate for H₂ was measured as $k_{\text{HF-H}_2} = (0.8 \pm 0.3) \times 10^7 \text{ sec}^{-1} \text{ Torr}^{-1}$. Time and funding did not permit more extensive self-relaxation or additive-relaxation measurements.

The temporal evolution of HF laser pulses was examined and compared with the vibrational fluorescence of the laser discharge and the temporal gain of the discharge. The importance of hydrogen in the discharge is discussed.

Reported observations of several resonant processes include bleaching, self-induced transparency, optical nutations, and an anomalous increase of 40 in the refractive index.

UNCLASSIFIED

SECURITY CLASSIFICATION OF THIS PAGE (When Data Entered)

PREFACE

An investigation of fundamental molecular processes in support of laser system design was begun for the Advanced Research Projects Agency under Contracts No. DAAH01-72-C-0573 and No. DAHC-15-67-C-0062 at the Environmental Research Institute of Michigan (ERIM), (formerly the Willow Run Laboratories of The University of Michigan). The effort currently reported, performed under Contract No. DAAH01-73-C-0591 and extending the earlier work, examines rotational energy between HF molecules.

Director of the program at ERIM is R.R. Legault. G. H. Lindquist served as Principal Investigator

The authors wish to thank Q. F. Carioti and R. A. Valade of ERIM for their able technical assistance.

CONTENTS

PREFACE	6
LIST OF ILLUSTRATIONS	6
1. INTRODUCTION AND SUMMARY	7
2. THE HF CHEMICAL LASER	11
2.1 Introduction	11
2.2 Power Supply	11
2.3 Laser Characteristics	13
2.3.1 Output Parameters	13
2.3.2 Laser Gain Experiment	20
2.3.3 Q-Switching Experiment	23
3. ROTATIONAL RELAXATION MEASUREMENTS	27
3.1 Introduction	27
3.2 Experimental Apparatus	29
3.2.1 Pockel's Cell	31
3.2.2 Gas Handling System	31
3.3 Experimental Results	34
3.3.1 Linear HF Absorption	34
3.3.2 HF Fluorescence—Vibrational Relaxation	36
3.3.3 Rotational Self-Relaxation of HF	38
3.3.4 Rotational Relaxation of HF by H ₂	44
4. RESONANCE PHENOMENA	45
4.1 Introduction	45
4.2 Self-Induced Transparency and Optical Nutations	45
4.3 Anomalous Propagation Velocity	46
REFERENCES	51
APPENDIX: THE RELATIONSHIP BETWEEN LASER PULSE SHAPE AND RELAXATION PROCESSES	53
DISTRIBUTION LIST	54

ILLUSTRATIONS

1. Triggering and Switching Circuit for Transverse-Discharge, Pulsed, HF Chemical "Pin" Laser	12
2. Energy Level Diagram of Vibration-Rotation-Excited HF	14
3. Fluorescence Radiation and Laser Radiation from HF Chemical Laser	15
4. Laser Output Power, Pulse Duration, and Total Energy for Various $P_1(J)$ Lasing Transitions	18
5. Far-Field Intensity Distribution of HF Laser Beam	19
6. Temporal Gain in HF Laser Discharge	21
7. Temporal Gain as a Function of Hydrogen Pressure for the $P_1(7)$ Laser Transition	24
8. Q-Switching as a Function of Delay Time	25
9. Optimum Q-Switched Pulse	26
10. Experimental Schematic for Rotational Relaxation Measurements	30
11. Electrical Switching of Pockel's Cell	32
12. Linear Absorption of HF Gas at 100°C for Several $P_1(J)$ Laser Transitions	35
13. Laser-Induced Fluorescence of HF Gas	37
14. HF Laser-Discharge Fluorescence	39
15. Oscilloscope Traces of Rotational Relaxation Measurements	41
16. Relaxation Time as a Function of Inverse Pressure	42
17. Observations of Optical Nutation	47
18. Observation of Radiation Propagation Velocity	49

ROTATIONAL RELAXATION MEASUREMENTS AND RESONANT PHENOMENA IN LASER-EXCITED HYDROGEN FLUORIDE

1

INTRODUCTION AND SUMMARY

Since the first demonstration of chemical lasing action in 1965 by Kasper and Pimentel [1], there has been much interest in producing a chemical laser with high output and maximum efficiency. Because the excitation energy is derived from the chemical reaction of the participating gases, the electrical efficiency can be high. All the chemical lasers developed to date operate in the infrared. Most are of the hydrogen-halide variety [2, 3], but the carbon monoxide chemical laser [4] and the CO₂ chemical transfer laser [5] have also received considerable attention. In the transfer laser, a chemical reaction provides vibrationally excited hydrogen (deuterium)-halide molecules, which transfer their energy to CO₂ molecules via collisions to produce lasing action at 10.6 microns.

The hydrogen-fluoride chemical laser has received the most attention. Several watts are obtainable in CW operation, tens of kilowatts are obtainable in a transverse pulsed discharge configuration, and several gigawatts have been obtained in 50 nsec pulses using electron beam excitation [6]. If one is to optimize lasing action, a thorough understanding of the various relaxation mechanisms is necessary. Vibrational-level lifetimes have been measured extensively using

-
1. J. V. V. Kasper and G. C. Pimentel, HCl Chemical Laser, *Phys. Rev. Letters*, **14**, pp. 352-54 (1965).
 2. T. F. Deutsch, Molecular Laser Action in Hydrogen and Deuterium Halides, *Appl. Phys. Letters*, **10**, pp. 234-36 (1967).
 3. K. L. Kompa and G. C. Pimentel, Hydrofluoric Acid Chemical Laser, *J. Chem. Phys.*, **41**, pp. 857-58 (1967) and A. N. Chester and L. D. Hess, Study of the HF Chemical Laser by Pulse-Delay Measurements, *IEEE J. Quant. Electr.*, QE-8, pp. 1-13 (1972), bibliography.
 4. C. Wittig, J. C. Hassler, and P. D. Coleman, Continuous Wave Carbon Monoxide Chemical Laser, *J. Chem. Phys.*, **55**, pp. 5523-32 (1971).
 5. D. J. Spencer, T. A. Jacobs, H. Mirels, and R. W. F. Gross, A Continuous Wave Chemical Laser, *Int. J. Chem. Kinetics*, **1**, pp. 493-94 (1969) and T. A. Cool, T. J. Falk, and R. R. Stephens, DF-CO₂ and HF-CO₂ Continuous-Wave Chemical Lasers, *Appl. Phys. Letters*, **15**, pp. 318-20 (1969).
 6. At the Sandia Laboratory — see, for example, *Electro-Optical Systems Design*, Nov. 1973, p. 6.

laser-induced fluorescence [7-9], and shock-tube techniques [10]. These showed that the self-relaxation rate of HF is on the order of $10^5 \text{ sec}^{-1} \text{ Torr}^{-1}$. Vibrational relaxation rates of HF as a result of the presence of various additive gases have also been measured [11].

Rotational relaxation is also of importance in the chemical laser rate equations but is more difficult to measure. Rotational relaxation is three orders of magnitude faster than vibrational relaxation, requiring experiments with submicrosecond response at mTorr pressures. Fluorescence radiation from a single vibration-rotation transition at these low pressures is very weak and precludes the use of laser-induced fluorescence to measure the rapid rotational relaxation rate.

However, laser-induced saturation followed by weak probing radiation to interrogate the excited system can be used at low gas pressures to measure rapid relaxation rates. An intense laser pulse can saturate the absorption of a single vibration-rotation transition. Since long-range collisions involving changes in the magnitude of the angular momentum provide the fastest relaxation mechanism, a measurement of the return of the saturated system back to rotational equilibrium will give the rotational relaxation rate of that transition.

The principal objective of this research program is to determine, using a laser pump-probe technique, the energy transfer rates of HF molecules by collisionally coupled changes in the magnitude of the rotational angular momentum.

The most relaxation information can be obtained by pumping on one vibration-rotation transition and probing on another. One may thus determine where and how rapidly the excitation energy is partitioned among the various rotational states of the excited vibrational level. In our HF rotational relaxation experiment, this required two HF lasers—a $P_1(J)^\dagger$ pump laser and $P_2(J')$ probe laser. For this technique to work, the probe must interrogate only that portion of the Doppler spectrum of the HF gas which is excited by the pumping radiation. The HF laser

7. J. R. Airey and S. F. Fried, Vibration Relaxation of Hydrogen Fluoride, *Chem. Phys. Letters*, **8**, pp. 23-26 (1971) and R. R. Stephens and T. A. Cool, Vibrational Energy Transfer and De-excitation in the HF, DF, HF-CO₂ and DF-CO₂ Systems, *J. Chem. Phys.*, **56**, pp. 5863-77 (1972).

8. R. M. Osgood, Jr., A. Javan, and P. B. Sackett, Measurement of Vibration-Vibration Energy Transfer Time in HF Gas, *Appl. Phys. Letters*, **20**, pp. 469-72 (1972).

9. J. K. Hancock and W. H. Green, Laser Excited Vibrational Relaxation Studies of HF, *J. Chem. Phys.*, **56**, pp. 2474-75 (1972).

10. J. F. Bott and N. Cohen, Shock Tube Studies of HF Vibrational Relaxation, *J. Chem. Phys.*, **55**, p. 3698 (1971) and J. F. Bott, HF Vibrational Relaxation Measurements Using Combined Shock-Tube, *J. Chem. Phys.*, **57**, pp. 96-102 (1972).

11. J. K. Hancock and W. H. Green, Vibrational Deactivation of HF ($v = 1$) in Pure HF and in HF-Additive Mixtures, *J. Chem. Phys.*, **57**, pp. 4515-29 (1972).

$^\dagger P_v(J)$ denotes the P-branch ($v - 1, J \rightarrow v, J - 1$) vibration-rotation transition.

linewidth, however, was found to be two orders of magnitude narrower than the Doppler spectral width, making frequency coincidence of the two lasers extremely difficult to achieve [12, 13].

The two-laser technique was therefore abandoned in favor of a single-laser technique whereby one laser pulse is divided into both pump and probe radiation. The first attempt involved splitting off part of the HF laser pulse, delaying it optically with a multiple-pass White cell, and returning it to the original beam to serve as the variable-delay probing radiation. The long tails of the HF laser pulses and the difficulty in obtaining long time delays, however, led to a second (and superior) single-laser technique.

A CdTe Pockel's cell was used as an optical switch to terminate the HF laser pulse abruptly and eliminate its long tail. The switching was not complete, however, and the weak 'leakage' radiation in the tail of the pulse served as the probing radiation. This method has the distinct advantage of having both pump and probe always collinear—there is no pump-probe beam alignment—and identical spectrally.

Relaxation measurements for several $P_1(J)$ HF transitions were made at gas pressures of several mTorr. The relaxation time was found to be inversely proportional to HF gas pressure as expected, with a rotational self-relaxation rate constant $k_{\text{HF-HF}}$ on the order of $10^8 \text{ sec}^{-1} \text{ Torr}^{-1}$. For the $P_1(J)$ transitions, however, where $J \leq 3$, the relaxation time was approximately constant with respect to HF pressure and is believed to result from the molecular transit time through the laser beam.

When He, air, or H_2 was added to the HF gas in the sample cell, the relaxation time, as would be expected, became shorter. The relaxation effect from the presence of the H_2 gas was measured and the rate constant $k_{\text{HF-H}_2}$ was determined to be $(0.8 \pm 0.3) \times 10^7 \text{ sec}^{-1} \text{ Torr}$. The large error is explained by the fact that this was a preliminary measurement and time did not permit a more accurate determination. It does, however, point out that the pump-probe method can be used effectively to measure the relaxation effects of additive gases.

During the investigation of relaxation processes in HF, several interesting complications developed. As mentioned above, the two-laser technique was found to be ineffective in performing the rotational relaxation experiment. This was because of the narrow spectral linewidth of the laser which was measured using time-resolved, bleachable, absorption of HF gas and found to be 3 MHz wide [12, 13]. This is 120 times narrower than the Doppler width and approaches the limit established by the laser pulse duration and the Heisenberg uncertainty principle.

12. L. M. Peterson, G. H. Lindquist, and C. B. Arnold, Rotational Relaxation and Self-Induced Transparency in HF Gas, Report No. 101300-17-P, Environmental Research Institute of Michigan, Ann Arbor, May 1974.

13. L. M. Peterson, C. B. Arnold, and G. H. Lindquist, Pulsed HF Chemical Laser Line-width Measurements Using Time Resolved Bleachable Absorption of HF Gas, *Appl. Phys. Letters*, **24**, pp. 615-17 (1974).

Several interesting nonlinear optical phenomena were also observed. When intense radiation "bleaches a hole" through an absorbing gas, the leading edge of the radiation pulse is attenuated until the absorbing transition has been saturated. Once this occurs, the rest of the pulse passes unattenuated. Our observations in HF, however, showed that the intensity of the trailing portion of the pulse was actually greater than that of the incident intensity—the transmission was in excess of 100 percent. This has been attributed to self-induced transparency [14] whereby radiation absorbed in the leading portion of the laser pulse is re-emitted later in the pulse. The transmission of the total energy of the laser pulse is anomalously high and is to be distinguished from the high transmission resulting from bleaching.

At the highest incident laser intensities, the waveform of the radiation passing through the absorbing HF gas exhibited damped oscillations. These oscillations have been identified as optical nutations [15]. They have an oscillation frequency which theory shows is linear with the laser E-field and are damped with a time constant equal to the homogeneous (collisional) relaxation time of the medium. This damping may provide a useful technique for measuring rotational relaxation times.

In addition, propagation velocities of laser radiation through the HF gas were observed to be 1/40 the speed of light—corresponding to a refractive index of 40.

Although these observations were incidental to the direct measurement of rotational relaxation in HF gas, the nonlinear optical processes themselves are highly dependent upon various relaxation mechanisms of the interacting gas and may be an even more valuable means of measuring relaxation rates. In addition, these processes may lead to: (1) lossless propagation through the atmosphere via self-induced transparency of absorbing water vapor; and (2) pulse steepening whereby laser pulses are compressed in time and increased in peak power as they propagate through an absorbing medium. These resonant phenomena contain some very interesting physical processes; with potential for providing valuable applications, they are certainly worthy of further study.

14. S. L. McCall and E. L. Hahn, Self-Induced Transparency by Pulsed Coherent Light, *Phys. Rev. Letters*, **18**, pp. 908-11 (1967) and Self-Induced Transparency, *Phys. Rev.*, **183**, pp. 457-85 (1969).

15. G. B. Hocker and C. L. Tang, Observation of the Optical Nutation Effect, *Phys. Rev. Letters*, **21**, pp. 591-94 (1968) and R. G. Brewer and R. L. Shoemaker, Photon Echo and Optical Nutation in Molecules, *Phys. Rev. Letters*, **27**, pp. 631-34, (1971)

THE HF CHEMICAL LASER

2.1 INTRODUCTION

The hydrogen fluoride chemical laser used in these experiments has been discussed previously [12, 16, 17]. It consisted of a transverse-discharge plasma tube with two rows of 40 pin-electrodes arranged in a single-turn, double helix. One row of electrodes was resistively loaded by 1 watt Allen Bradley carbon resistors, $910\ \Omega$ each; the other row was connected with a common bus strap. Electrode separation was about 1cm. The Lucite plasma tube was 0.2 m long and had Brewster-angle sapphire windows whose crystal axes were oriented such that no change of laser polarization occurred. Hydrogen and sulfur-hexafluoride were used as reactant gases in quantities $H_2:SF_6$ of from 1:20 to 10:20 Torr. It was found that the sapphire windows remained cleanest when the gas mixture entered directly opposite the window and exited at the center of the discharge tube.

The laser cavity was comprised of a $625\ \ell/\text{mm}$, $2.85\ \mu\text{m}$ blazed grating for single laser line operation; a 1.5mm aperture; and a 1m radius, 50% reflecting, gold-coated, infrared-quartz output mirror (an uncoated Ge flat was occasionally used). The laser was designed to provide stable, reproducible, laser pulses with a minimum of time jitter with respect to the trigger signal. Emphasis was placed upon spectral, spatial, and temporal uniformity of the pulses in order to obtain a workable, controllable laser to perform the experimental investigations with a minimum of extraneous variables. This end was achieved, but not without a sacrifice in output power and energy. Typical output while operating at 5:20 Torr of $H_2:SF_6$ and capacitors charged to 20 kV, was a peak power of 10 watts, a power density of $500\ \text{W}/\text{cm}^2$ and an energy of about 5 μjoule per pulse. The output varied from line to line and varied with $H_2:SF_6$ pressure (see Section 2.2.1).

2.2 POWER SUPPLY

As shown in Figure 1, energy for the laser discharge was supplied by four 500 pF doorknob capacitors charged to 20 kV and connected in parallel to reduce the inductance. The capacitors, hydrogen thyatron, shunting resistor, and trigger circuit were mounted in a Faraday cage directly on top of the laser discharge tube in order to minimize electrical interference. By keeping the connectors as short as possible, stray inductance is reduced and maximum energy is delivered to the discharge. The hydrogen thyatron, although its voltage and current limitations

16. G. H. Lindquist et al., Investigations of Chemical Laser Processes, Report No. 191300-1-P, Environmental Research Institute of Michigan, Ann Arbor, February 1973.

17. G. H. Lindquist et al., Investigations of Chemical Laser Processes, Report No. 191300-2-F, Environmental Research Institute of Michigan, Ann Arbor, June 1973.

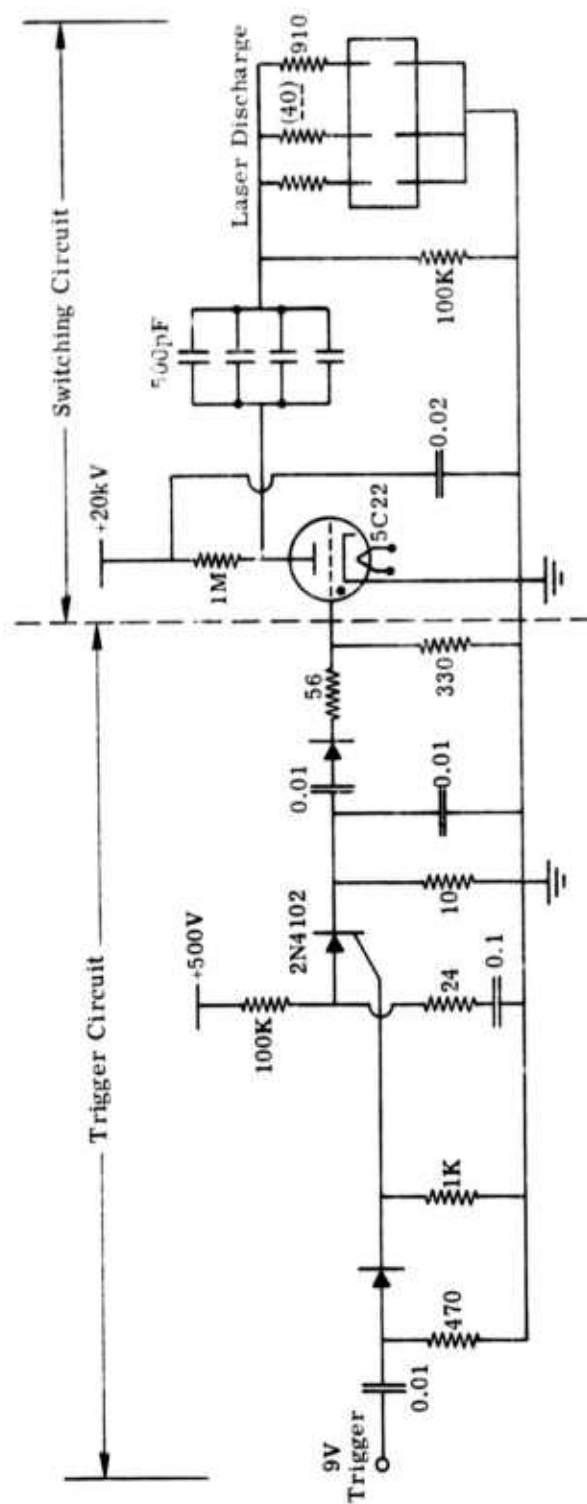


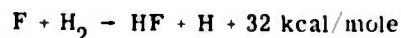
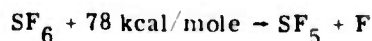
FIGURE 1. TRIGGERING AND SWITCHING CIRCUITS FOR TRANSVERSE-DISCHARGE, PULSED, HF CHEMICAL "PIN" LASER. Resistors in ohms, capacitors in μ F unless specified.

are much lower than those for spark gaps, was chosen because of its low time-jitter and long-life time. Our present system has operated for over 500 hours at a repetition rate of about 5 pps. Electrical pulse jitter is only a few nanoseconds although the onset of lasing action, which occurs approximately 800 nsec after the 60 nsec electrical discharge (see Section 2.3.1), has a time jitter of about 10 nsec.

Various storage capacitors from 0.0015 to 0.1 μF were used to drive the discharge. Peak laser power output did not change but pulse duration, and therefore total energy, increased with increasing capacitance. When the capacitance exceeded 0.05 μF , however, the electrical discharge was long enough that arcing occurred. Laser pumping then ceased and the rest of the energy stored in the capacitors was wasted.

2.3 LASER CHARACTERISTICS

Operation of the HF chemical laser is most easily visualized with the aid of Figure 2. An electrical discharge produces atomic fluorine from the SF_6 gas (or other fluorine donors such as the freons). When the atomic fluorine unites with the hydrogen from the H_2 gas (or other hydrogen donors such as the $\text{C}_n\text{H}_{2n+2}$), this exothermic reaction yields 32 kcal/mole of excess energy



which appears in the form of vibrationally excited HF^* and kinetic energy. Since rotational relaxation is very rapid, the molecules appearing in a particular vibrational level will be quickly partitioned into a Boltzmann distribution through collisions. Therefore, the population in each J-state decreases with increasing J value (except of course for J very small; e.g., $J < 2$ at normal temperatures) and a "partial inversion" exists between \bar{J} -states in an upper vibration level and J-states in a lower vibrational level when J is greater than \bar{J} . Since the selection rule $\Delta J = \pm 1$ specifies the allowed transitions, a partial inversion may lead to lasing action with $\Delta J = +1$, or the $P_v(J)$ transitions. $R_v(J)(\Delta J = -1)$ lasing transitions due to partial inversion occur for the low J values ($J < 2$ for HF). The strongest lasing transitions are the $P_1(2) - P_1(9)$ and $P_2(2) - P_2(9)$. Weaker lasing action occurs for the $P_3(J)$ transitions [2, 18] and for $P_v(J)$ transitions where J can be as high as 15 [2, 18].

2.3.1 OUTPUT PARAMETERS

Figure 3(a) shows oscilloscope traces of the high voltage electrical pulse from the power supply which excites the laser discharge; it also shows traces of the fluorescence signal

18. O. R. Wood and T. Y. Chang, Transverse-Discharge Hydrogen-Halide Lasers, Appl. Phys. Letters, 20, pp. 77-79 (1972).

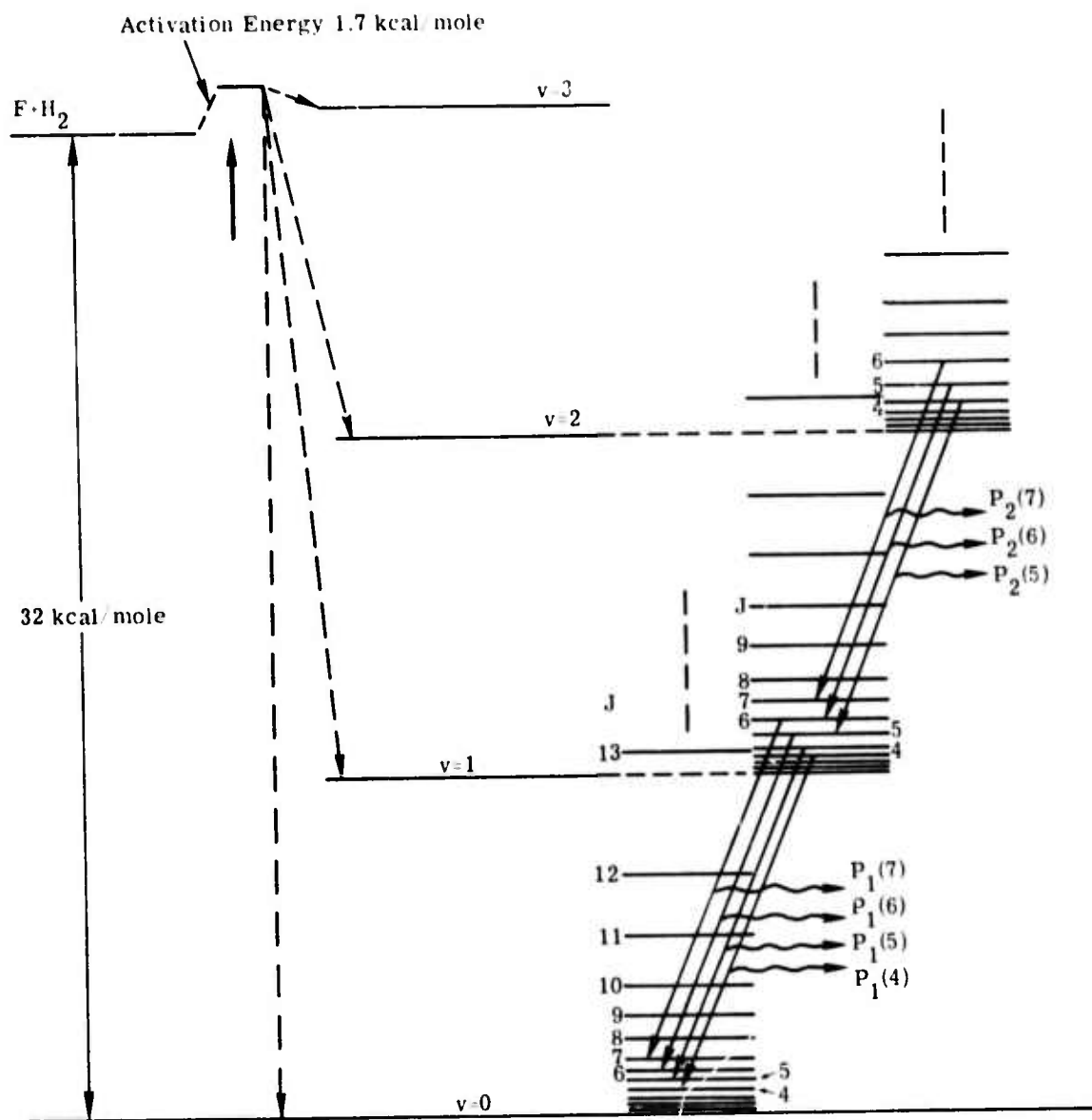
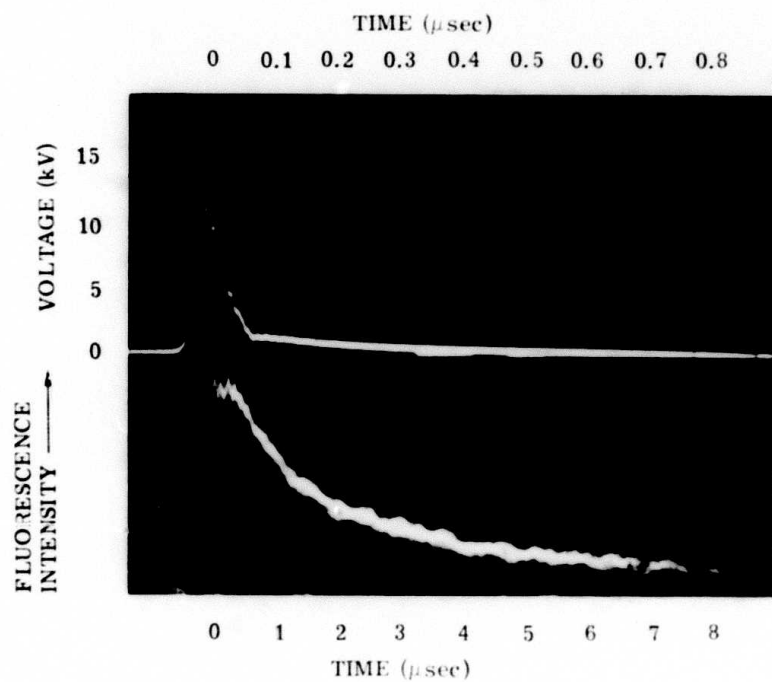
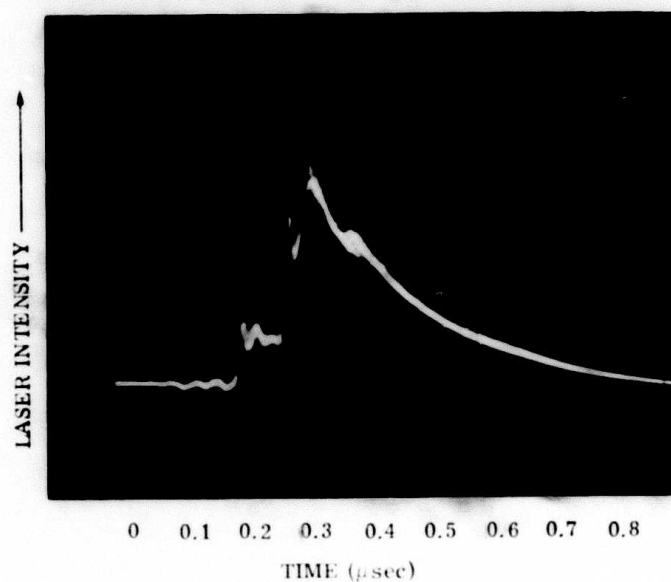


FIGURE 2. ENERGY LEVEL DIAGRAM OF VIBRATION-ROTATION - EXCITED HF.
Laser action is shown for several $P_1(J)$ and $P_2(J)$ transitions.



(a) High-Voltage Electrical Pulse to Laser and Resulting Fluorescence Radiation from Excited HF in Discharge. $\text{H}_2:\text{SF}_6 = 5:20$ Torr.

FIGURE 3. FLUORESCENCE RADIATION AND LASER RADIATION FROM HF CHEMICAL LASER. All waveforms are a superposition of about 20 traces. (Continued)



(b) Multiple-Line Laser Radiation. Without a grating for tuning, both $P_1(J)$ and $P_2(J)$ transitions lase together. $H_2:SF_6 = 5:20$

FIGURE 3. FLUORESCENCE RADIATION AND LASER RADIATION FROM HF CHEMICAL LASER. All waveforms are a superposition of about 20 traces. (Concluded)

radiated by the discharge. The electrical pulse lasts for only 60 nsec but the fluorescence lasts for several microseconds with a $\text{H}_2:\text{SF}_6$ ratio of 5:20 Torr—the fluorescence time decreases with increasing H_2 pressure (see Section 3.3.2 and Ref. [11]).

Figure 3(b) shows oscilloscope traces of the laser output when a 100% reflecting mirror (in place of the grating) and the 50% output mirror form the laser cavity. The first pulse is due to lasing action of the $\text{P}_2(\text{J})$ transitions and the second pulse is composed of both $\text{P}_1(\text{J})$ and $\text{P}_2(\text{J})$ transitions. The first $\text{P}_2(\text{J})$ pulse appears as a result of the partial inversion existing between the J-states of the $v = 2$ and $v = 1$ levels, and lasing action persists until the lower states fill and the inversion no longer exists. A partial inversion now exists between the J-states of the $v = 1$ and $v = 0$ levels, causing $\text{P}_1(\text{J})$ laser emission. Since this depletes the $v = 1$, J-states, lasing action may again occur for the $\text{P}_2(\text{J})$ transition, and a cascading effect occurs between the $v = 2$ and $v = 0$ levels.

Figure 4 shows the variation in output peak power, pulse duration, and energy for several $\text{P}_1(\text{J})$ transitions when the laser is in single-line operation (i.e., grating present). This particular data was taken with $\text{H}_2:\text{SF}_6$ pressures of 5:20 Torr and an electrical pulse of 17 kV. Although energy increases with J, peak power decreases. This occurs because of the rapid increase in pulse duration with increasing J.

The peak laser power was largely a function of SF_6 pressure and almost independent of H_2 pressure. As SF_6 pressure increased, the output power increased; as H_2 pressure increased, the peak output power increased very slightly until a pressure was reached (at approximately $\text{H}_2:\text{SF}_6 = 1:1$) where lasing abruptly ended.

Pulse duration, on the other hand, was largely a function of H_2 pressure and independent of SF_6 pressure. With 20 Torr of SF_6 , the pulse duration ($1/e$) went from a minimum of about 40 nsec to about 1 μsec as the H_2 pressure decreased from about 20 Torr down to 0.5 Torr (see gain dependence as a function of H_2 pressure in Section 2.3.2).

The near- and far-field patterns of the laser beam were scanned with a 0.02 mm^2 InAs detector. The far-field pattern was examined at the focus of a 50cm lens and is shown in Figure 5. The top trace is intensity versus time of the $\text{P}_1(6)$ pulses; the bottom one is intensity as a function of lateral position in the far-field beam with increments of 0.187mm. The full-angle divergence at half-intensity is 2.2 mrad and is close to the diffraction limit of 1.9 mrad determined* from the 1.5mm limiting aperture of the HF laser.

The smooth, divergence-limited beam would indicate TEM_{00} operation as would the extremely narrow spectral linewidth of the laser which was measured [12, 13] to be 3 MHz.

*The angular radius to the first minimum of an Airy pattern is $\theta = 1.22 \lambda/D$ where D is the aperture diameter. The angular diameter at half intensity is $\theta = 1.02 \lambda/D$.

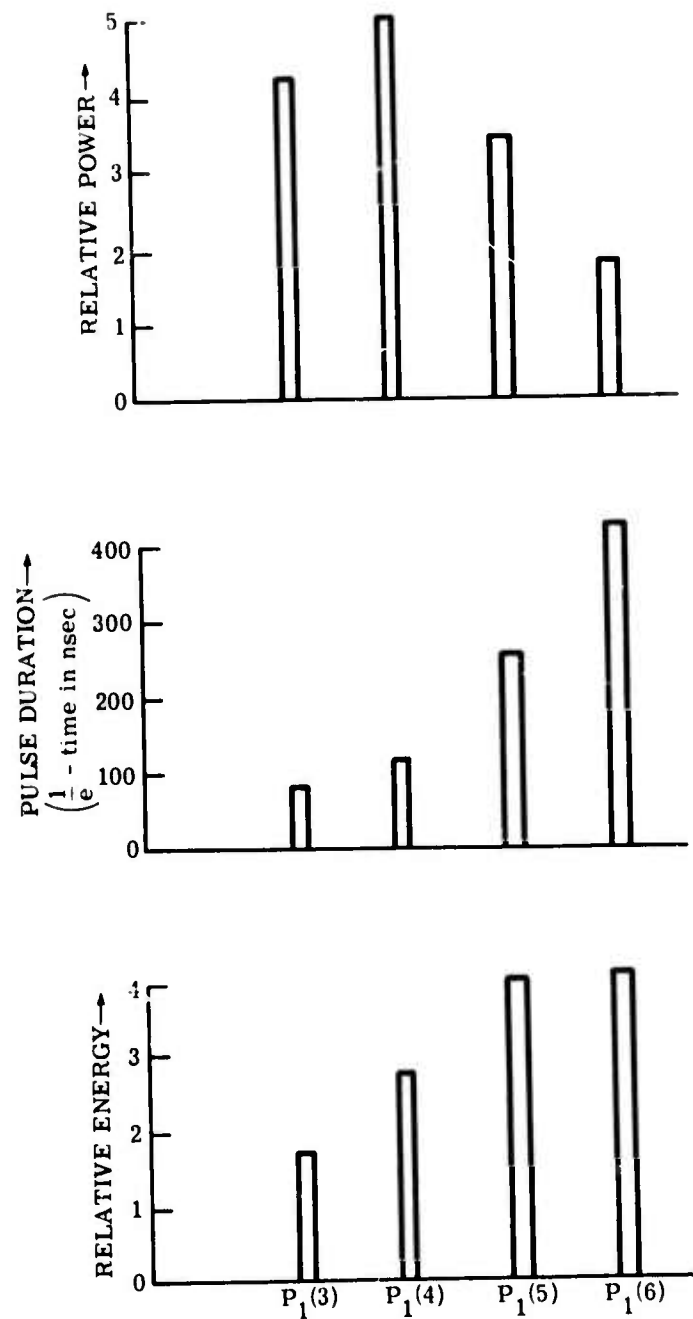


FIGURE 4. LASER OUTPUT POWER, PULSE DURATION, AND TOTAL ENERGY FOR VARIOUS $P_1(J)$ LASING TRANSITIONS.

$H_2:SF_6 = 5:20; 17kV$

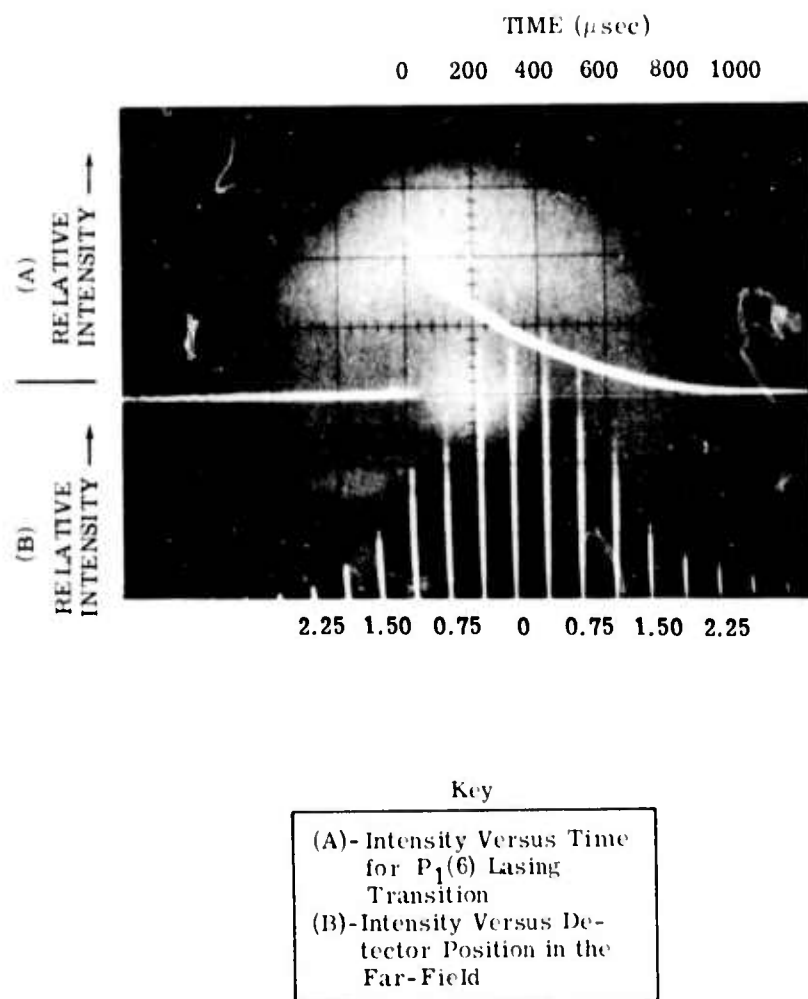


FIGURE 5. FAR-FIELD INTENSITY DISTRIBUTION OF HF LASER BEAM

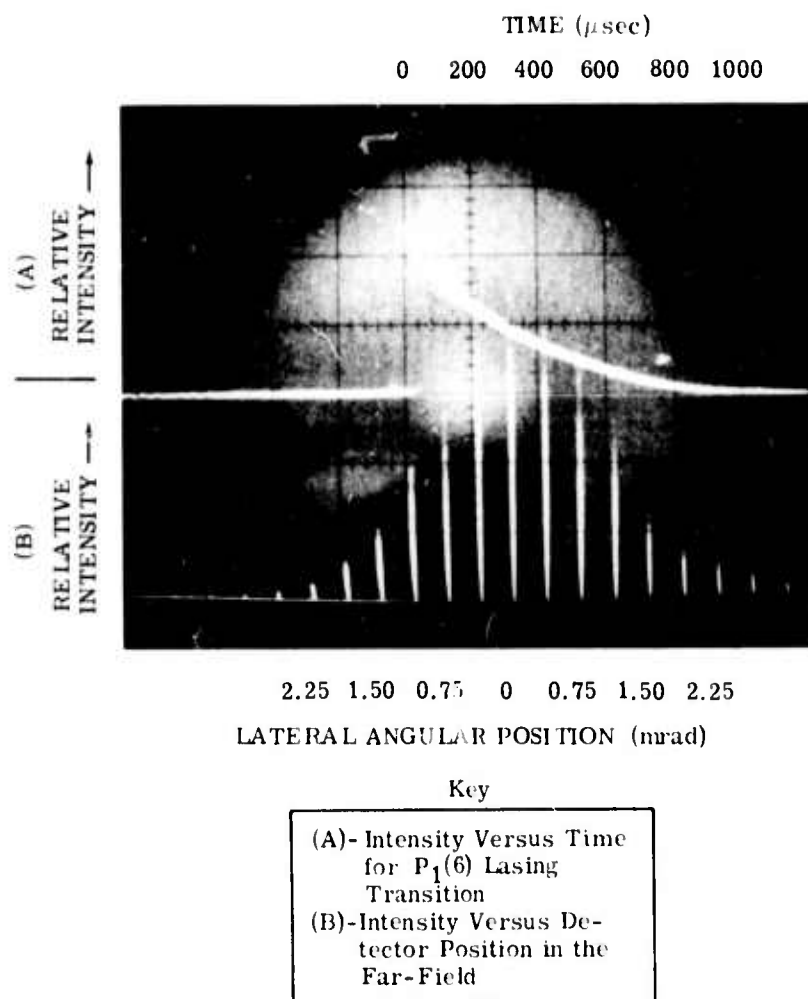


FIGURE 5. FAR-FIELD INTENSITY DISTRIBUTION OF HF LASER BEAM

When two separate lasers were beat together (heterodyning), the beat-note was constant in frequency throughout the pulse, indicating no frequency 'chirping' [12, 13]. The beat-note did not seem to change as the detector was moved to different parts of the beam, thus demonstrating spatial as well as temporal spectral purity of the laser pulses. The beat-note did change smoothly from pulse to pulse however, indicating frequency drift with time, which is presumably due to thermal and mechanical changes in the optical cavity (i.e., changes in cavity length and mirror/grating angles).

2.3.2 LASER GAIN EXPERIMENT

The gain exhibited by the HF laser transverse discharge was cursorily examined. This experiment, though by no means complete, proved valuable in understanding the temporal evolution of the laser pulses and may be of value in determining relaxation parameters of the active HF gas. Our results, which are in agreement with gain measurements in pulsed HF lasers using the intercavity attenuation technique [19] and the single-pass gain method [20], complement these measurements by providing additional time-resolution of both gain and relaxation for the excited states.

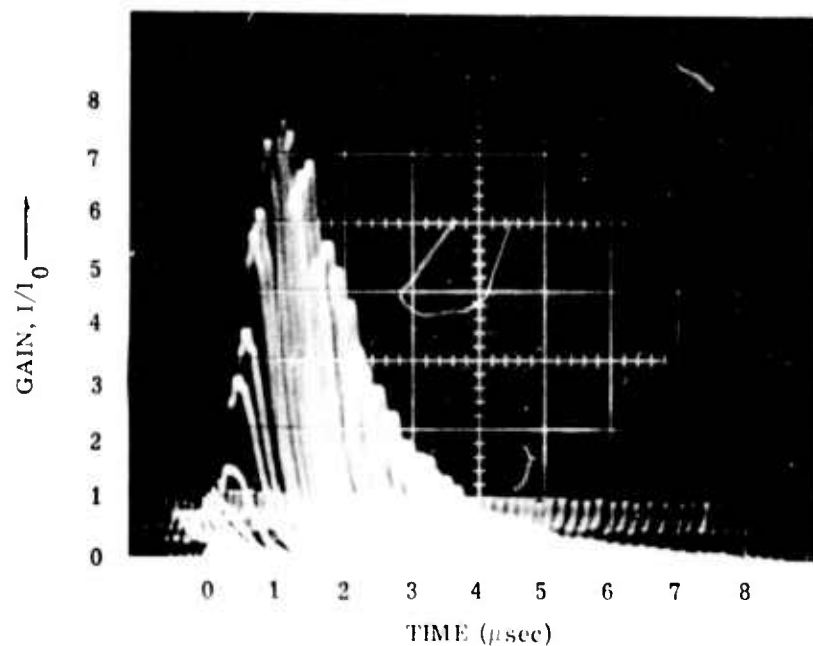
The gain of our 0.2 m laser plasma tube was determined by passing suitably attenuated radiation from a second HF laser through the discharge and observing the amplification. The onset of the interrogating laser pulse could be varied in time with respect to the high voltage discharge to the plasma tube by triggering off of the variable time delay of a Tektronix 556 oscilloscope.

Figure 6 shows several oscilloscope traces of gain (or loss) as a function of time. The 60 nsec electrical pulse to the 0.2 m amplifier begins at $t = 0$. Each recorded pulse represents the amplified signal at a different delay time for a particular $P(J)$ transition. The gain increases rapidly after the electrical discharge, reaches a peak, then decreases at a slower rate until, beyond several microseconds, it becomes less than one (i.e., attenuation). For reactant pressures $H_2:SF_6$ of 5:20 Torr and an electrical pulse of 18 kV, the gain for $P_1(5)$ probing radiation maximizes at about 1 μ sec and decreases for about 3 μ sec beyond this peak as may be seen in Figure 6(a). The buildup to maximum gain ($I/I_0 = 8$) corresponds to the observed several-hundred-nanosecond delay of the HF laser's $P_1(J)$ pulses. The $P_1(J)$ laser pulse duration is less than the fall time of the gain; this is presumably a result of the depletion of the upper lasing level by the lasing action itself.

19. C. R. Jones, Gain and Energy Measurements on an Electrically Pulsed Chemical Laser, *Appl. Phys. Letters*, 22, pp. 653-55 (1973).

20. S. Marcus and R. J. Carbone, Gain and Relaxation Studies in Transversely Excited HF Lasers, *IEEE J. of Quant. Electr.*, QE-8, pp. 651-55 (1972).

(a) Gain for $P_1(5)$
Transition;
 $G = 10\%/cm$



(b) Gain for $P_2(4)$
Transition;
 $G = 17\%/cm$;
Vertical Scale
Has Been Ex-
panded 20 Times
for Pulses at
the Right

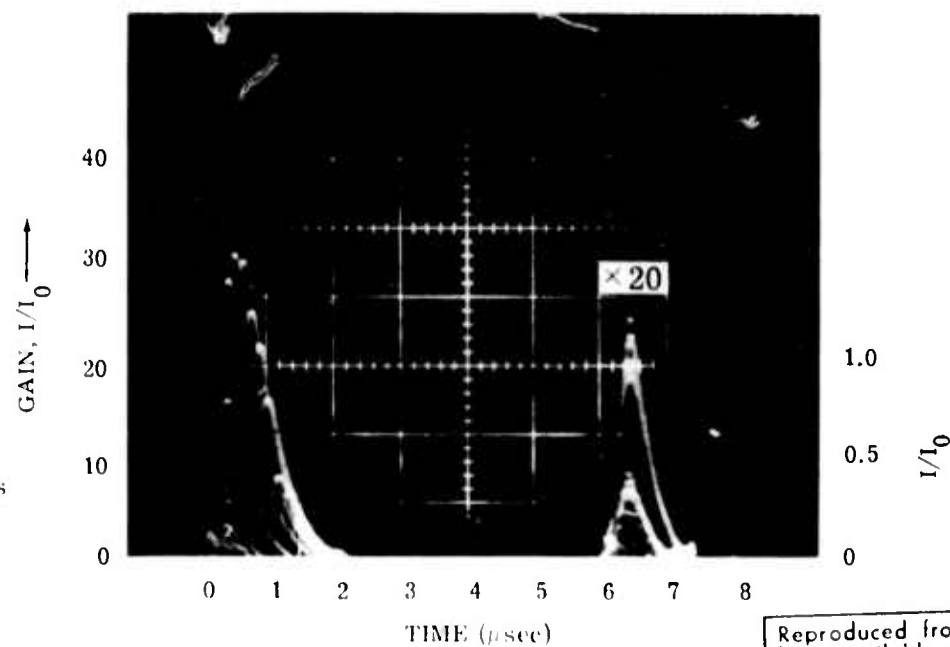
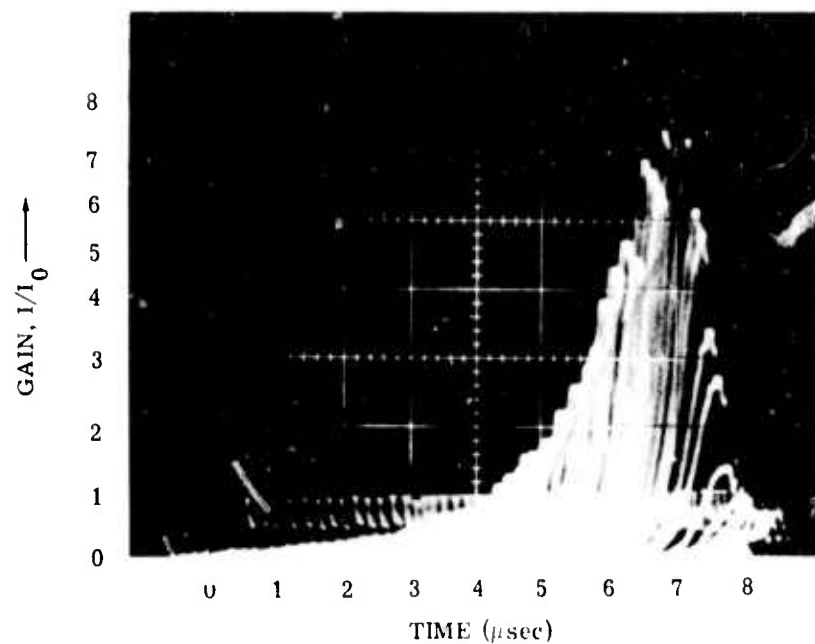


FIGURE 6. TEMPORAL GAIN IN HF LASER DISCHARGE. $H_2:SF_6 = 5:20$; 18 kV.
Note that $I/I_0 < 1$ denotes absorption. (Continued)

Reproduced from
best available copy.



(a) Gain for $P_1(5)$
Transition;
 $G = 10\%/cm$



(b) Gain for $P_2(4)$
Transition;
 $G = 17\%/cm$;
Vertical Scale
Has Been Ex-
panded 20 Times
for Pulses at
the Right

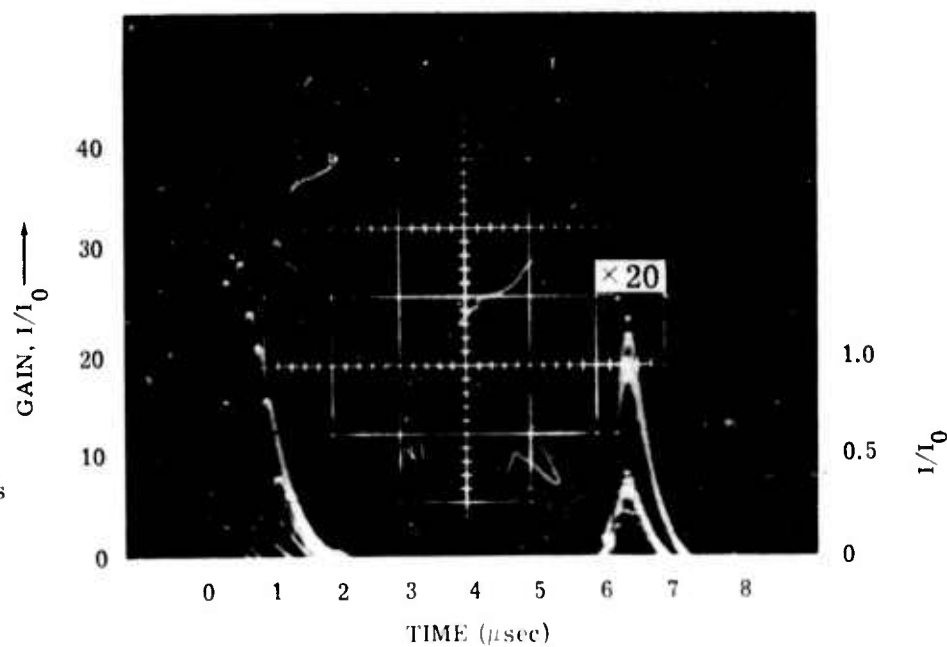
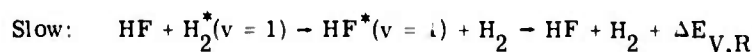
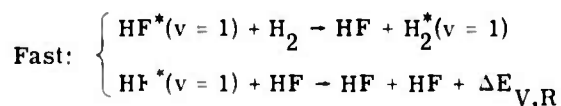


FIGURE 6. TEMPORAL GAIN IN HF LASER DISCHARGE. $H_2:SF_6 = 5:20$; 18 kV.
Note that $I/I_0 < 1$ denotes absorption. (Continued)

Figure 6(b) shows gain as a function of time for the $P_2(4)$ transition. Here, gain is greater ($I/I_0 = 30$), reaches a maximum sooner, and decays more rapidly than for the $P_1(5)$ measurement. This is in qualitative agreement with observations of HF laser pulses wherein $P_2(J)$ transitions are more intense, have a shorter delay time, and are of shorter duration than the $P_1(J)$ laser pulses.

In addition to gain, Figure 6 parts (b) and (c) show attenuation for the longer delay times (the vertical sensitivity has been increased 20-fold). In particular, the absorption of the $P_2(4)$ radiation is a monitor of the population of the first excited vibrational level of HF in the discharge tube (or more precisely, the population difference between the $v = 2$ and $v = 1$ levels). The transmission of the HF gas to $P_2(4)$ radiation increases exponentially (approximately) from an initial value of 0.3 with a time constant of about 58 μsec . This is presumably due to the relaxation of the excited HF molecules from the first vibrational level.

It is interesting to compare Figure 6(a) and 6(c), since the $P_1(5)$ and $P_2(4)$ lasing transitions share a common $v = 1, J = 4$ state. From (c), the $1/e$ deactivation time of the $v = 1$ level (implied by the decreasing absorption of the $P_2(4)$ transition) is about 58 μsec (we assume rotational equilibrium exists throughout this process). In (a) however, the gain has ceased and strong absorption occurs within a few μsec , indicating not only the loss of inversion but also the depopulation or deactivation of the $v = 1$ level (again assuming rapid rotational equilibrium). It would appear that two relaxation mechanisms are at work. The fastest would correspond to collisional deactivation of vibrationally excited HF due to self-relaxation ($k_{\text{HF-HF}}^v = 5.7 \times 10^4 \text{ sec}^{-1} \text{ Torr}^{-1}$; see Section 3 and reference [11]) or H_2 relaxation ($k_{\text{HF-H}_2}^v = 2.4 \times 10^4 \text{ sec}^{-1} \text{ Torr}^{-1}$ [11]). The slow relaxation time may be explained by the trapping effect of the H_2 gas [11, 21]. Since the first vibrational levels of HF and H_2 are nearly resonant, the H_2 may carry away the vibrational energy of HF through $v-v$ transfer collisions. The excited H_2 eventually returns the vibrational energy to HF which, in turn, may be deactivated via self-relaxation. The trapping effect has a time constant much longer than that for self-relaxation.



21. H. Chen and C. B. Moore, Vibration-Vibration Energy Transfer in Hydrogen Chloride Mixtures, J. Chem. Phys., 54, pp. 4080-84 (1971).

H_2^* self-relaxation is very slow and may be neglected ($k_{\text{H}_2-\text{H}_2}^v = 1.2 \text{ sec}^{-1} \text{ Torr}^{-1}$) [22]. It may be noted that the slow relaxation is not simply due to flushing out of the HF by the vacuum pump. The flush rate was observed using the change of $\text{P}_1(5)$ absorption with time and found to be several msec—in agreement with the pump rate of the fore pump.

Figure 7 shows how gain changes with H_2 pressure in the discharge tube for the $\text{P}_1(7)$ transition. The 60 nsec electrical pulse occurs at $t = 0$ and the amplified signal is obtained from a number of traces similar to those shown in Figure 6. Excess H_2 gas can be seen to produce a rapid fall-off of gain with time. The lower vibrational levels of H_2 are nearly resonant with those of HF and are therefore very effective in relaxing vibrational excited HF [11]. However, excess H_2 also means that more HF is being produced [23] and self-relaxation is more effective than HF- H_2 relaxation [11]. Although more excited HF is produced for lasing action, a point is reached at which self-relaxation dominates. Thus there is an optimum pressure for maximum output in an HF laser [20].

2.3.3 Q-SWITCHING EXPERIMENT

The CdTe Pockel's cell used in the rotational relaxation measurements of HF (see Section 3.2.1) was placed inside the cavity of the 0.2 m HF laser to provide a variable delay Q-switch. The Pockel's cell optical switch was in a crossed polarizer configuration which spoiled the laser cavity Q until a high-voltage (half-wave voltage) step opened the 'switch' to allow lasing action. The onset of the voltage pulse was adjustable in time by use of the variable delay in our oscilloscope. Trace (A) of Figure 8 shows the 18 kV electrical pulse to the laser discharge; trace (B) shows the laser pulse without optical switching. No lasing action occurred for 800 nsec after the electrical pulse. Trace (C) shows the effects of Q-switching upon the laser output. As the onset of lasing action is forced to later times, the peak intensity increases, reaches a maximum, and decreases all the while the pulse duration steadily decreases.

Trace B in Figure 9 shows Q-switched pulses at a fixed delay time with peak power at a maximum. Each trace in Figures 8 and 9 comprises the superposition of about 20 pulses each, showing good reproducibility. The peak power of the Q-switched pulse is 2.3 times that of the unswitched pulse, is about two-thirds as energetic, and has a pulse width which is shorter by about a factor of five. Each laser pulse appears to be broken up into three portions. Careful examination of the Q-switched pulse shows a sharp spike at the leading edge (the peak extends above the baseline of the electrical pulse, A), followed by an intermediate decay and then by a very gradual decay to zero. These features may be seen in the unswitched pulses as well as

22. F. DeMartini and J. Ducuing, Stimulated Raman Scattering in Hydrogen: A Measurement of the Vibrational Lifetime, *Phys. Rev. Letters*, **17**, pp. 117-19 (1966).

23. W. H. Beattie, G. P. Arnold, and R. G. Wenzel, Chemical Efficiency in a Pulsed HF Laser, *Chem. Phys. Letters*, **16**, pp. 164-68 (1972).

(c) Decay of $P_2(4)$ Absorption Showing Vibrational Relaxation of $V = 1$ Level. Set of Traces Taken Under the Same Conditions as (b) Above but with an Expanded Time Scale

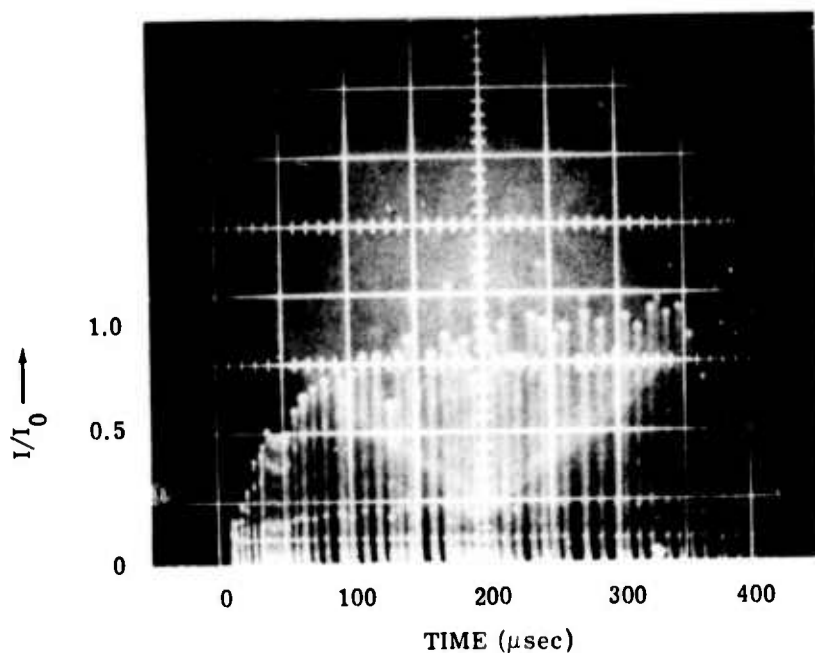


FIGURE 6. TEMPORAL GAIN IN HF LASER DISCHARGE. $H_2:SF_6 = 5:20$; 18 kV.
Note that $I/I_0 < 1$ implies absorption. (Concluded)

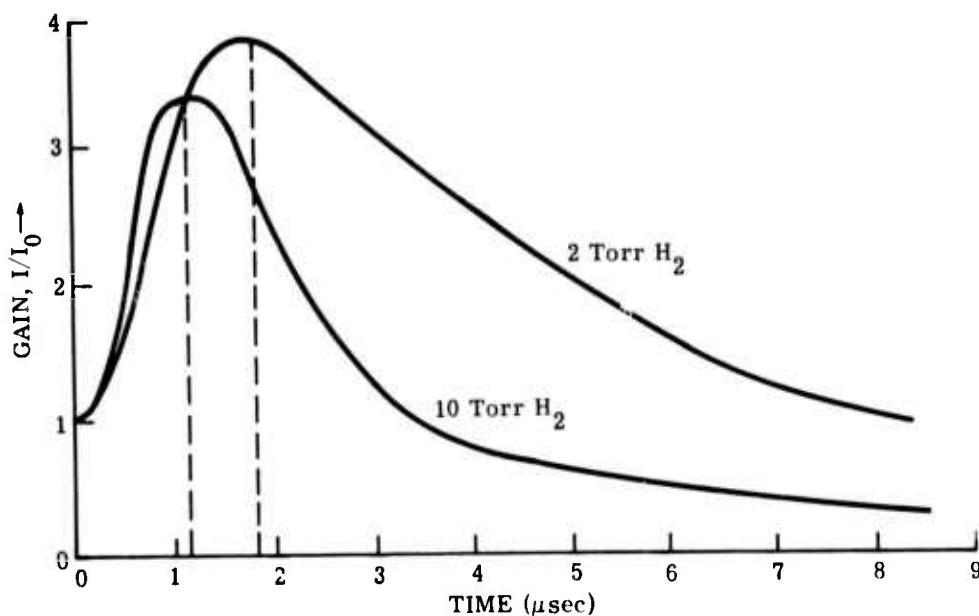


FIGURE 7. TEMPORAL GAIN AS A FUNCTION OF HYDROGEN PRESSURE FOR $P_1(7)$ LASER TRANSITION. $SF_6 = 20$ Torr.

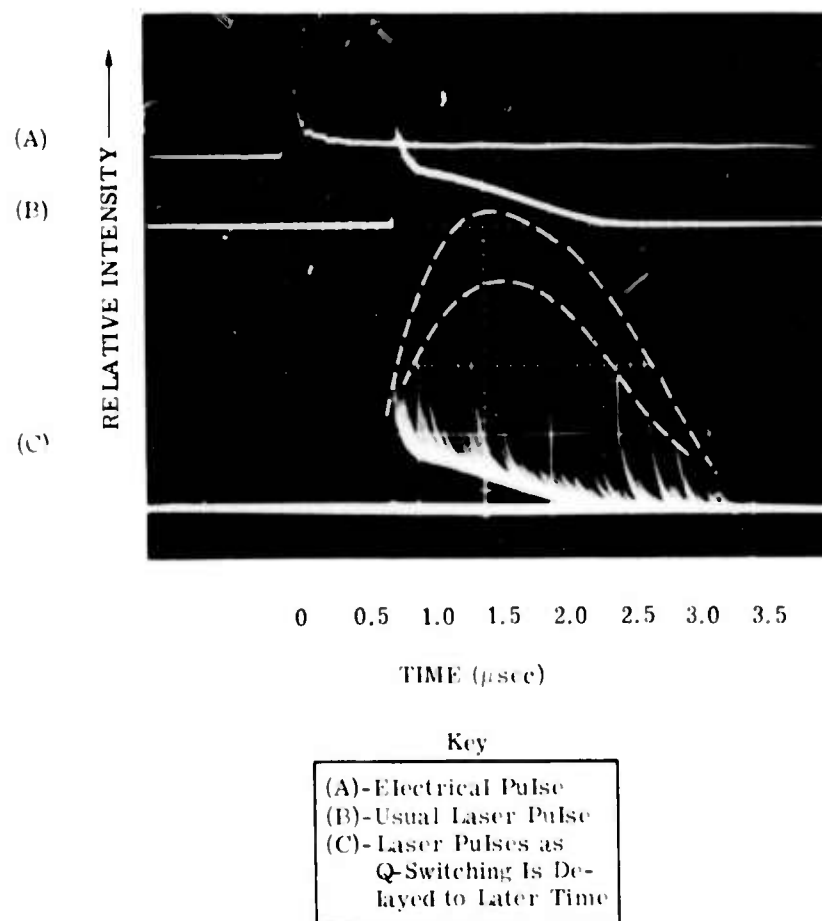


FIGURE 8. Q-SWITCHING AS A FUNCTION OF DELAY TIME

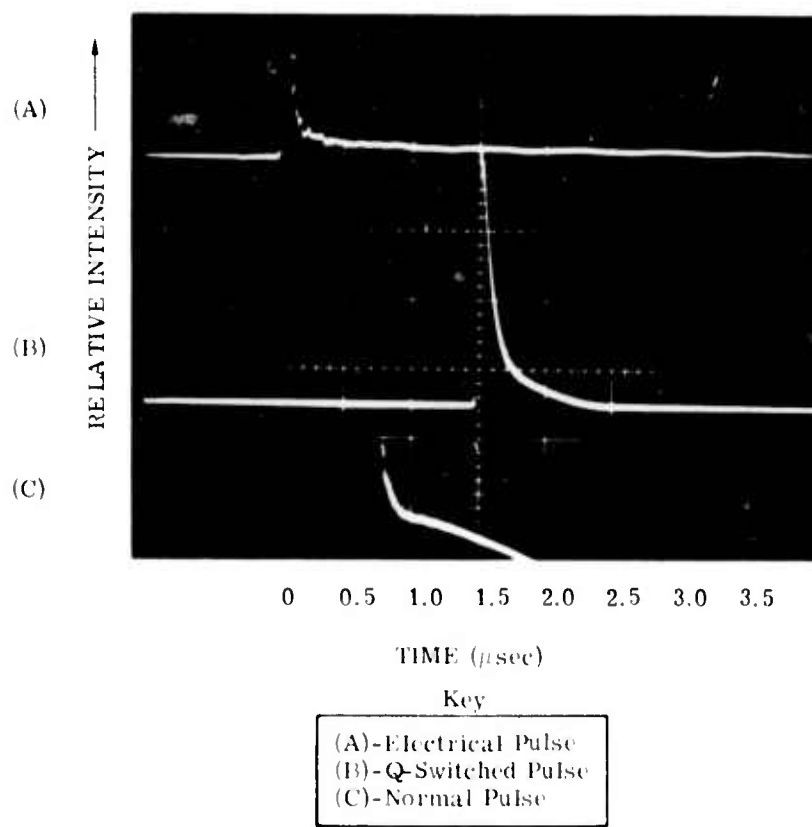


FIGURE 9. OPTIMUM Q-SWITCHED PULSE

the Q-switched pulses, and are particularly noticable in trace (C) of Figure 8. The first feature, which corresponds to the rapid-rise, rapid-fall spike, is difficult to see in reproduction but has been outlined with dashes. The second corresponds to the intermediate decay; the third corresponds to the slowest decay and coincides exactly with the tail of the unswitched pulse.

The similarity between the Pockel's Q-switched pulses and the unswitched pulses, with particular regard to their rapid rise-time and large delay, leads one to suspect self-Q-switching of the latter. This is quite likely since the presence of ground-state HF in the laser cavity allows Q-switching through saturable absorption, i.e., lasing action will not commence until a spectral 'hole' has been bleached through the absorbing gas. Similarly, Q-switching of the $P_v(J)$ levels is possible due to the population of the excited v, J -state within the laser cavity. This self-Q-switching or spectral 'hole-burning' may help to explain the extremely narrow 3 MHz laser linewidth measured in our laboratory [12, 13].

3

ROTATIONAL RELAXATION MEASUREMENTS

3.1 INTRODUCTION

The principal objective of this research program was to determine the energy transfer rates of molecules excited to a particular vibration-rotation level by long range dipole-dipole collisions involving changes in the magnitude of the rotational angular momentum. As mentioned above (see Section 1) the two-laser pump-probe (double-resonance) approach was unsuccessful in measuring these relaxation rates because of the extremely narrow spectral linewidth of the pulsed HF 'pin' lasers [12, 13] and the resulting absence of spectral coincidence between the pump and the probe lasers. Since the pump laser (operating on a $P_1(J)$ transition) is very narrow, spectrally, only those molecules in the Doppler velocity distribution which are resonant with the radiation will be excited. To interrogate this excited, non-equilibrium condition, the probe radiation must also be resonant with the narrow spectrum of excited molecules. Even when the excited molecules undergo collisions involving changes in J and the probing occurs at a vibration-rotation level different from that initially excited, the same narrow component of the Doppler velocity distribution is maintained (translational relaxation is an order of magnitude slower than rotational relaxation [24]) and the problem of spectral coincidence still exists.

Consider $P_1(J - 1)$ pumping radiation. Since the laser is 120 times narrower than the Doppler spectral width [12, 13], only those HF molecules in the Doppler distribution of the $v = 0, (J - 1)$ -state which have velocity components in resonance with the radiation will be excited. A narrow 'hole' will be bleached in the lower $v = 0, (J - 1)$ -state approximately equal to the spectral linewidth of the laser, and a corresponding 'spectral-spike' of molecules will occur in the excited $v = 1, J$ -state. Since rotational relaxation involving changes in $|J|$ are three

24. F. J. Zelzenik and R. A. Svehla, Rotational Relaxation in Polar Gases, J. Chem. Phys., 53, pp. 632-46 (1970).

orders of magnitude faster than vibrational relaxation [7-10], this 'spectral spike' will be distributed with time into the various other J' states within the first excited state. Rotational energy transfer occurs primarily by long range multipolar interactions which do not substantially change the translational energy of the molecules involved. This is the reason that rotational relaxation is much faster than translational relaxation, and insures that the narrowness of the 'spectral spike' and its position within the Doppler velocity distribution of the J' -state will be maintained even though the molecules change J -states.

In order to interrogate the population of the J' -state in the first excited vibrational level, the $P_2(J')$ probe laser must also be spectrally narrow and coincide exactly with the 'spectral spike' of excited molecules in the J' -state. The pulse-to-pulse frequency instabilities of pulsed HF lasers in conjunction with their extremely narrow spectral linewidth make this technique very difficult.

The two-laser approach was abandoned in favor of a single-laser approach whereby a single laser pulse is separated into both a strong pumping portion followed by a weak probing portion, thus alleviating the problem of spectral coincidence. A limitation of the single-laser approach is the loss of flexibility to probe on transitions other than the pumped transition.

The separation of a single laser pulse into both pump and probe was first accomplished using an optical-delay White cell and, secondly, with a Pockel's cell optical switch. Preliminary rotational relaxation measurements were made and appear in the Semi-Annual Report of this contract [12]. The single-laser approach using the Pockel's cell was modified slightly during the second half of the contract period to produce more consistent relaxation times with a minimum of error.

A brief HF fluorescence experiment was also performed and the vibrational relaxation rate obtained was found to agree with reported values [11]. The single-laser pump-probe technique was used to measure the rotational relaxation time of HF as a function of HF gas pressure in the mTorr range. Self-relaxation rates were obtained as were relaxation rates of HF caused by the presence of hydrogen as an additive gas. (Rotational relaxation measurements of CO_2 have been made in CO_2 laser discharges using pump-probe techniques [25] similar to those used here.)

25. P. K. Cheo and R. L. Abrams, Rotational Relaxation Rate of CO_2 Laser Levels, Appl. Phys. Letters, 14, pp. 47-9 (1969) and Collisional Relaxation of CO_2 Rotational Levels by N_2 and He, Appl. Phys. Letters, 15, pp. 177-78 (1969); R. R. Jacobs, S. J. Thomas, and K. J. Pettipiece, J-Dependence of Rotational Relaxation in the CO_2 00^0_1 Vibrational Level (to appear in IEEE J. of Quant. Electr., 1974); and T. O. Carroll and S. Marcus, A Direct Measurement of the Rotational Relaxation Time in CO_2 , Phys. Letters, 27A, pp. 590-91 (1968).

3.2 EXPERIMENTAL APPARATUS

The experimental configuration used to measure rotational relaxation times in HF gas is illustrated in Figure 10. The HF laser was of helical transverse 'pin' discharge design [12, 16, 17] and was 0.2 m in length with sapphire Brewster windows whose optic axes were oriented such that no polarization rotation occurred. The cavity was 37 cm long with a 1.5 mm limiting aperture, a 625 ℓ /mm grating blazed at $\lambda 2.85 \mu\text{m}$ for single laser-line operation, and an infrared quartz mirror (with a 1 m radius of curvature), gold-coated for 50% reflectivity at $\lambda 2.7 \mu\text{m}$ to provide output coupling. The calcite Polarizers (Optical Instruments Inc.) P_1 , P_2 and P_3 were of the Glann-Thompson variety and were oriented for vertical, horizontal, and vertical polarizations, respectively, as indicated in the figure. The Pockel's cell (manufactured by II-VI, Inc.) was a single CdTe crystal ($5 \times 5 \times 40 \text{ mm}$) with silver-deposited electrodes and an anti-reflection coating for $\lambda 3 \mu\text{m}$ (see Section 3.2.1).

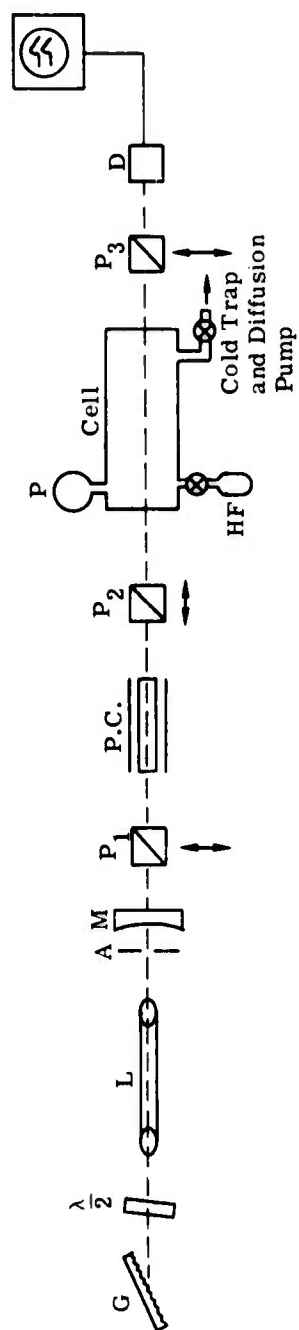
The fast, 0.02 mm^2 , InAs photovoltaic detector (Jodon Engineering Associates), D, was used and back-biased at 1.6 V for maximum time response. The detector was limited by the response time of the Tektronix 556 oscilloscope with a 1A1 preamplifier which had a measured response of 2.4 nsec.

In the absence of an applied electric field to the Pockel's cell, almost all of the laser radiation is extinguished by the crossed polarizer P_2 (extinction $\sim 10^{-3}$). Application of a 200 nsec, 1.7 kV square wave to the CdTe crystal provided half-wave retardation at $\lambda 2.7 \mu\text{m}$ which rotated the plane of polarization of the laser radiation from vertical to horizontal such that the radiation was transmitted by the polarization analyzer, P_2 .

The high-voltage pulse to the Pockel's cell was triggered from the same trigger pulse that fired the laser. The onset of the high-voltage pulse could be fine-tuned by varying the amplitude of the trigger pulse until the Pockel's cell on-time coincided with the leading portion of the laser pulse. Thus, the laser pulse was transmitted unattenuated by polarizer P_2 for the first 200 nsec and, when the high-voltage pulse terminated, was extinguished for the duration of the laser pulse.

Polarizer P_2 was oriented to pass horizontally polarized radiation, but, since it was not perfect, a small amount of vertically polarized radiation 'leaked' through. This radiation was weaker by about three orders of magnitude than the unattenuated laser pulse and served as the probing radiation.

Intense pumping radiation during the first 200 nsec drove the absorbing transition of the HF gas in the cell into saturation. Pumping then ceased, and the probe radiation interrogated the transition for the duration of the laser pulse. Relaxation of the saturated condition appeared as an increase in the absorption of the probe radiation with time.



Key:

- G - Grating
- $\lambda/2$ - Saphire half-wave plate
- L - Laser "pin" discharge
- A - 1.5mm aperture
- M - 50% R output mirror
- P_{1,2,3} - Polarizers (specified orientation)
- P.C. - Pockel's cell
- P - Capacitance manometer
- D - InAs detector

FIGURE 10. EXPERIMENTAL SCHEMATIC FOR ROTATIONAL RELAXATION MEASUREMENTS

The polarizer P_3 , oriented to block pump radiation but pass probe radiation, prevented the detector D from being driven into saturation by the intense exciting radiation. It should be noted that the HF gas is pumped with horizontally polarized radiation and probed with orthogonal vertically polarized radiation. This is of no consequence since we are dealing with a gas which rotates through many cycles ($\sim 10^{12}$ Hz) within the duration of the laser pulse. Though the exciting radiation is vertically polarized, excited dipoles appear quickly in all directions.

It may also be noted that because of slight defects in the birefringence of the CdTe crystal, a small amount of horizontally polarized radiation is present along with the vertically polarized probing radiation. Its intensity is on the same order as that of the probing intensity and is of no consequence.

3.2.1 POCKEL'S CELL

The CdTe electro-optic modulator was a single crystal ($5 \times 5 \times 40$ mm) with $110 \times \bar{1}10 \times 001$ orientation. Ends were polished and anti-reflection coated for $\lambda 3 \mu\text{m}$ (compromise between the $\lambda 2.7 \mu\text{m}$ HF laser and $\lambda 3.5 \mu\text{m}$ DF laser), and the $\bar{1}10$ sides were deposited with silver electrodes. When the cell was placed between crossed polarizers, its transmission T varied according to

$$T = \sin^2\left(\frac{\pi}{2} \frac{V}{V_{\lambda/2}}\right)$$

where V is the voltage applied to the crystal

$V_{\lambda/2}$ is the voltage which provides half-wave retardation

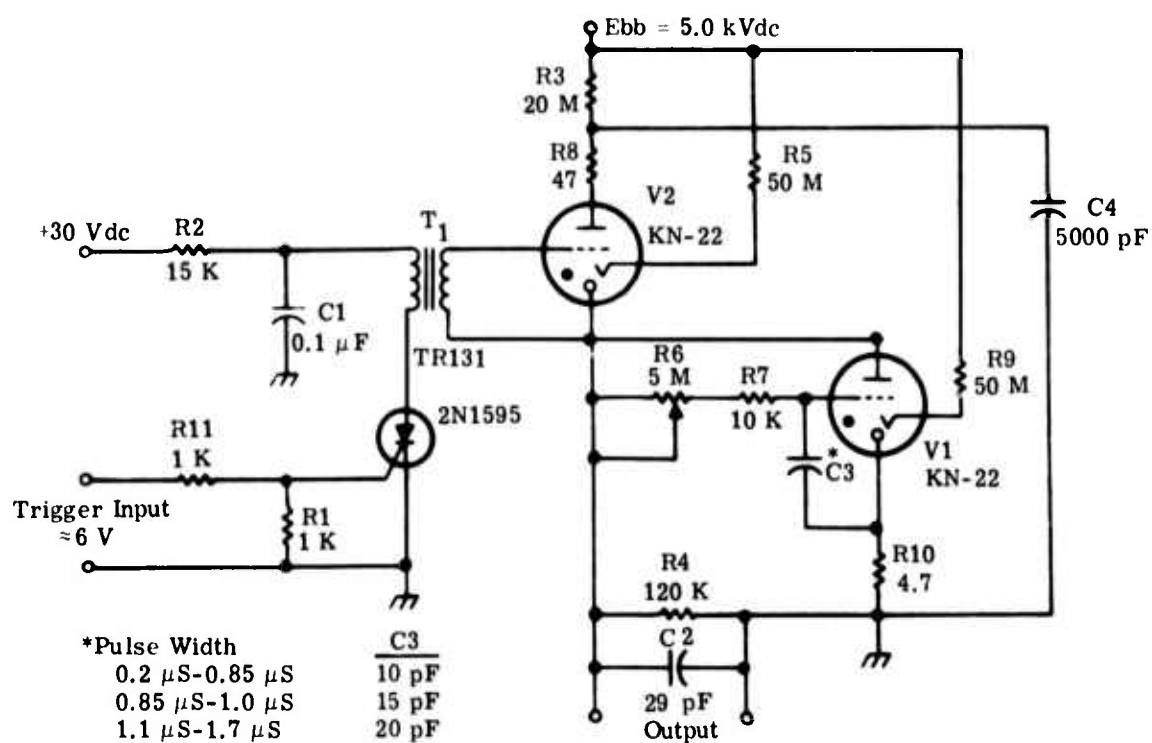
For $\lambda 2.7 \mu\text{m}$, $V_{\lambda/2}$ was measured as 1.7 kV.

The high-voltage should be applied in the form of short pulses with small duty cycle to prevent crystal breakdown and consequent damage. Figure 11 shows the electronic schematic of the high-voltage square-wave generator using krytron (EG&G) switch tubes and the resulting electrical pulse which drove the electro-optic crystal. Electrical switching time is on the order of 20 nsec, although it should be noted that the optical switching time should be even faster because of the sine-squared dependence of optical transmission upon voltage (the crystal response time is on the order of picoseconds).

As mentioned above, the position of the pulse in time could be finely-tuned by varying the amplitude of the triggering pulse. To keep electrical leads as short as possible and minimize electrical interference picked up by the oscilloscope, the square-wave generator circuitry was mounted inside a metal shield on the optical carrier holding the CdTe crystal.

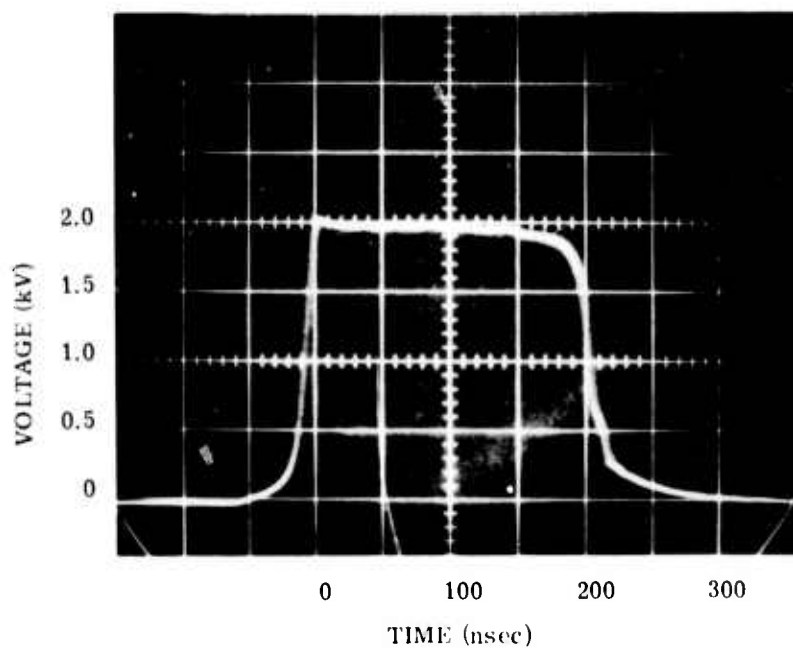
3.2.2 GAS HANDLING SYSTEM

The HF gas absorption cell was made of Monel as were the HF cylinder and connective tubing. The Baratron capacitive manometer, P, in Figure 10 was HF-resistant and was sensitive from 1 to 10^3 mTorr. The HF cylinder was maintained at -85°C to freeze out impurities



(a) Schematic Diagram, Krytron Pulse Generator

FIGURE 11. ELECTRICAL SWITCHING OF POCKEL'S CELL (Continued)



(b) High-Voltage Square Wave at CdTe Pockel's Cell

FIGURE 11. ELECTRICAL SWITCHING OF POCKEL'S CELL (Concluded)

(particularly water) and the cylinder was exposed to a high vacuum for approximately 15 minutes before each use. Most experiments were performed under flowing gas conditions to avoid uncertainties in HF pressure resulting from absorption of HF on the container walls. Experiments performed under static, nonflowing conditions gave identical results except for the measurements involving additive gases. When gases other than HF were introduced into the cell at pressures (several hundred mTorr) sufficient to affect the HF relaxation, the flow rate through the cell was reduced because of the limited capacity of the vacuum pump. The pressure ratio of HF and the additive gas was uncertain in such cases, and, for them, a static, nonflowing system was used.

3.3 EXPERIMENTAL RESULTS

The first two subsections below present measurements of HF absorption and HF fluorescence lifetime. The results are not new but the experiments performed were a good starting point for our relaxation measurements in HF. Agreement of the data with published and theoretical results helped assure us as to the accuracy of our work. The final two subsections present and discuss the relaxation measurements toward which this investigation was directed.

3.3.1 LINEAR HF ABSORPTION

The absorption of HF gas at several $P_1(J)$ vibration-rotation transitions was measured by simply passing radiation from the tuneable HF laser through the gas cell and recording the decrease in transmission with varying HF pressures. It is important that the laser radiation be sufficiently attenuated so that the gas medium responds linearly. Figure 12 presents the transmission of the HF gas at 100°C to several lasing transitions as a function of gas pressure. The data points were determined experimentally and the straight lines were calculated from the expression

$$\alpha = \frac{B(0,J; 1, J - 1)}{c \gamma_D^{1/2}} \left(\frac{\ln 2}{\pi} \right)^{1/2} N(2J + 1) \frac{hcB_0}{kT} \exp \left[- \frac{hcB_0}{kT} J(J + 1) \right]$$

where $B(0,J; 1, J - 1)$ is the Einstein B for the $P_1(J)$ transition

γ_D is the Doppler full-width at half-height

$\tilde{\nu}$ is the frequency in wavenumbers

N is the molecular number density

J is the rotational quantum number of the lower state

T is the gas temperature

B_0 is the rotational constant for the $v = 0$ vibrational level

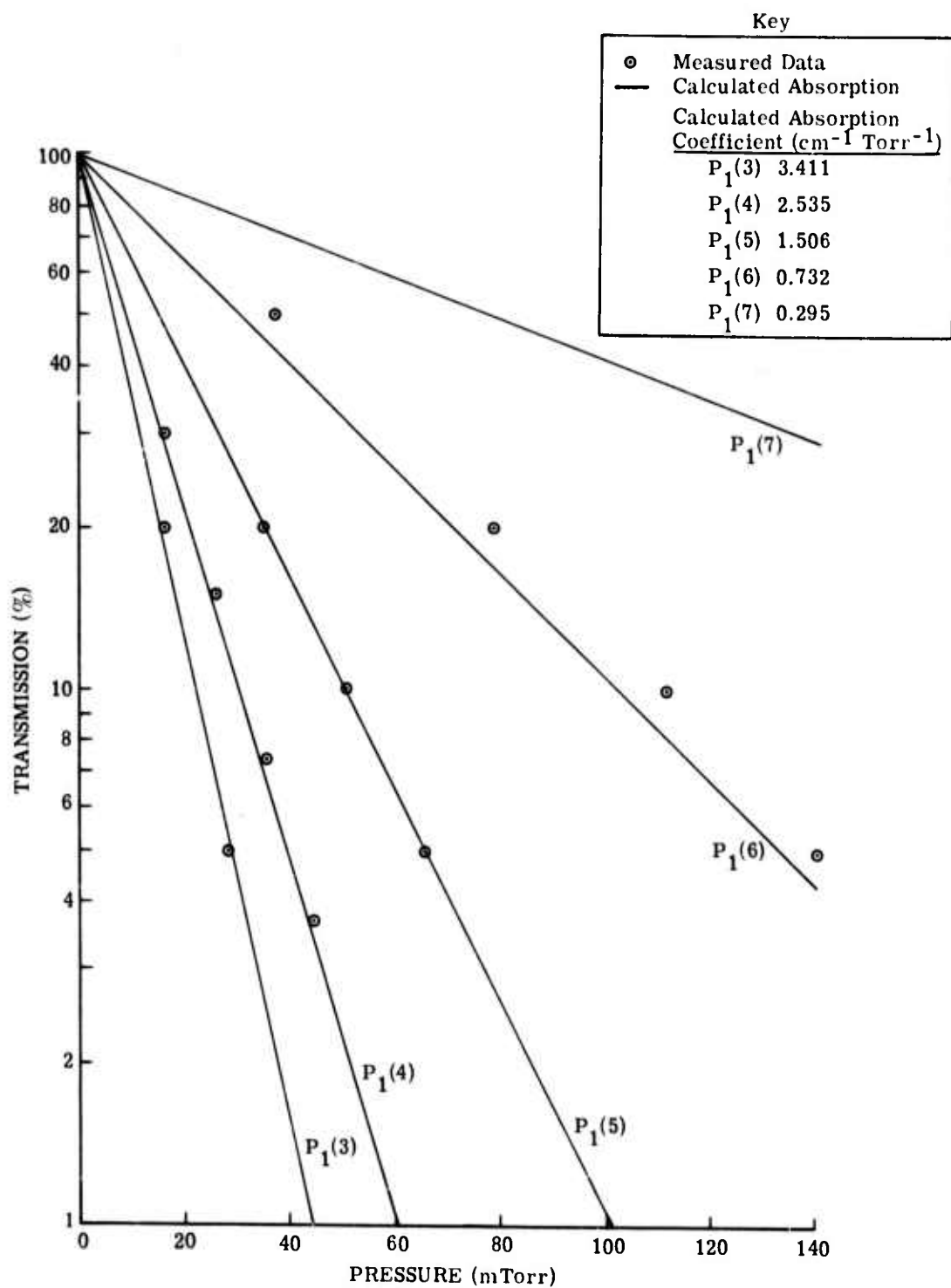


FIGURE 12. LINEAR ABSORPTION OF HF GAS AT 100°C FOR SEVERAL $P_1(J)$ LASER TRANSITIONS

The $B(v, J; v', J')$ were determined using the Einstein A [26] and the relation $B = A / 8\pi \nu^2$. The excellent agreement obtained between theory and experiment indicates that the laser is operating very close to the Doppler line center.

3.3.2 HF FLUORESCENCE — VIBRATIONAL RELAXATION

From copper tubing we constructed a small gas cell 58mm long and 14mm in diameter with an entrance and exit gas port, and thin glass windows. A slot was machined in the side of the tube parallel to its axis for side viewing of fluorescence radiation. Radiation from the side window, detected with a liquid-nitrogen-cooled InSb photovoltaic detector, was amplified with a fast, integrated circuit, video amplifier and displayed on an oscilloscope. With the cell evacuated, scattered radiation from the laser pulses provided a strong signal for the detector. When HF was added to the cell, however, the scattered intensity was reduced to a barely detectable level. In addition, the scattered signal occurred only during the microsecond duration of the laser pulse and did not affect the longer fluorescence lifetime measurement.

Figure 13 shows an oscilloscope trace and corresponding logarithmic plot of the fluorescence signal provided by 0.44 Torr of HF in the cell at room temperature when irradiated with $P_1(4)$ laser pulses. The decay of the fluorescence is clearly exponential with a time constant of 51.0 μsec . The vibrational self-relaxation rate of $k_{\text{HF-HF}}^v (=1/\tau_p)$ is $4.46 \times 10^4 \text{ sec}^{-1} \text{ Torr}^{-1}$, in agreement with previously reported results at room temperature [11]. This relaxation rate, however, is not in agreement with values obtained at higher temperatures [7, 10] or in the presence of dilute argon with HF at room temperatures [11] where $k_{\text{HF-HF}}^v$ is measured as $8.7 \times 10^4 \text{ sec}^{-1} \text{ Torr}^{-1}$. (Dilution in Ar reduces such effects as temperature rise during excitation, and relaxation by collisions with the cell walls, without affecting the vibrational self-relaxation time of HF [11, 21]). It was suggested [11] that the slower relaxation rate in pure HF at room temperature may be a result of nonequilibrium of the rotational degree of freedom during vibrational self-relaxation of HF. Our results, presented below (Section 3.3.3), indicate that complete rotational relaxation occurs in the time scale and pressure range of the vibrational relaxation measurements.

It is interesting to compare the fluorescence of pure, laser-excited HF with the fluorescence of the HF laser discharge itself (see Figure 3(a) of Section 2.2.i). In both cases, the fluorescence comes from vibrationally excited HF gas; but in the laser discharge, the presence of gases other than HF (in particular H_2) tends to modify the fluorescence considerably.

26. R. E. Meredith and F. G. Smith, Investigations of Fundamental Laser Processes, II, Computation of Electric Dipole Matrix Elements for HF and DF, Report No. 84130-39-T(II), Willow Run Laboratories, The University of Michigan, Ann Arbor, November 1971.

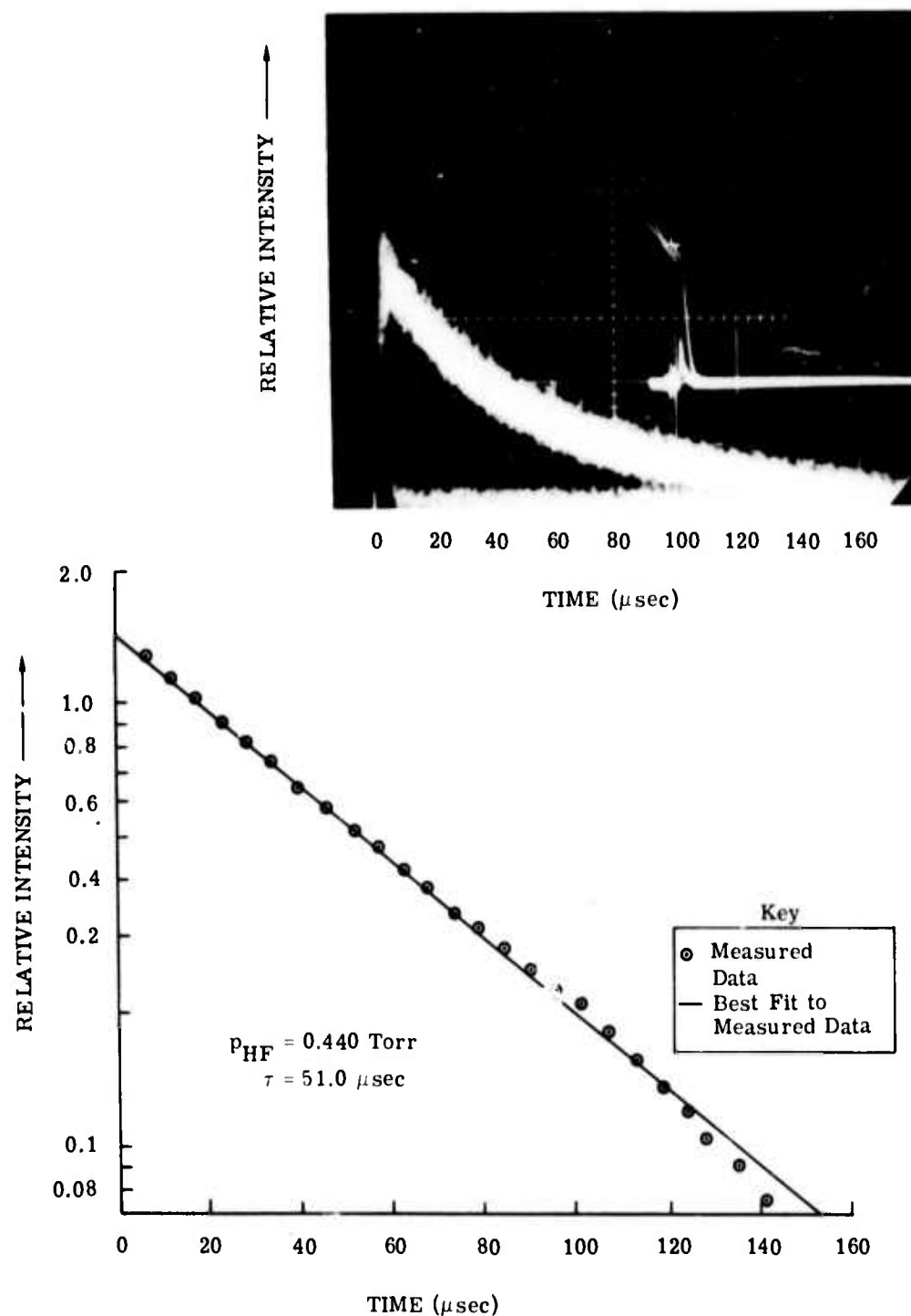


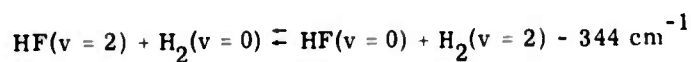
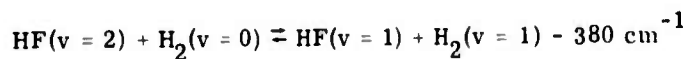
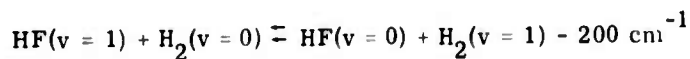
FIGURE 13. LASER-INDUCED FLUORESCENCE OF HF GAS

Figure 14 is a logarithmic plot of fluorescence intensity as a function of time taken from Figure 3(a). It is certainly more complex than the simple exponential of Figure 11. The intensity relationship with time may be separated into a sum of exponentials, with a fast τ_f and slow τ_s time constant [11, 21].

$$\frac{I}{I_0} = e^{-t/\tau_f} + e^{-t/\tau_s}$$

The τ_s may be obtained by extrapolating a straight line from the data at large t . Subtracting this line from our observed data results in a linear set of points whose slope is a measure of the fast relaxation time τ_f .

The fast relaxation time represents the deactivation of vibrationally excited HF by HF and H_2 . A near-resonance condition exists between the lower vibrational levels of HF and H_2



such that H_2 collisions ($V \rightarrow V$) are effective in relaxing HF; $k_{HF-H_2}^v = 2.4 \times 10^4 \text{ sec}^{-1} \text{ Torr}^{-1}$ [11]. However, the relaxation ($V \rightarrow R, T$) rate of H_2 itself is small, $k_{H_2-H_2}^v = 1.2 \text{ sec}^{-1} \text{ Torr}^{-1}$ [11, 22], such that the vibrationally excited H_2 eventually returns its energy back to the HF gas. This return of vibrational energy to the HF molecules results in the slow time-constant of Figure 14.

Unfortunately, the effect of H_2 gas upon lasing action is to rapidly couple energy out of the vibrationally excited HF and reduce the lasing output power; yet the coupling of energy from the H_2 back into HF is not fast enough to build up much of an inversion, if any, and restore the lost energy to the laser pulse.

The relaxation effects from the near resonance of H_2 and HF would explain the increased laser energy output (approximately double) when H_2 is replaced by methane, ethane, or propane in the laser discharge.

3.3.3 ROTATIONAL SELF-RELAXATION OF HF

Rotational relaxation measurements of a single laser-excited vibration-rotation level were made using a time resolved pump-probe technique. (The experimental configuration was discussed in Section 3.2 above.) Laser pulses were shaped using the CdTe Pockel's cell before passing through the 0.3 m HF gas cell at 100°C and onto the fast InAs detector. The first 200

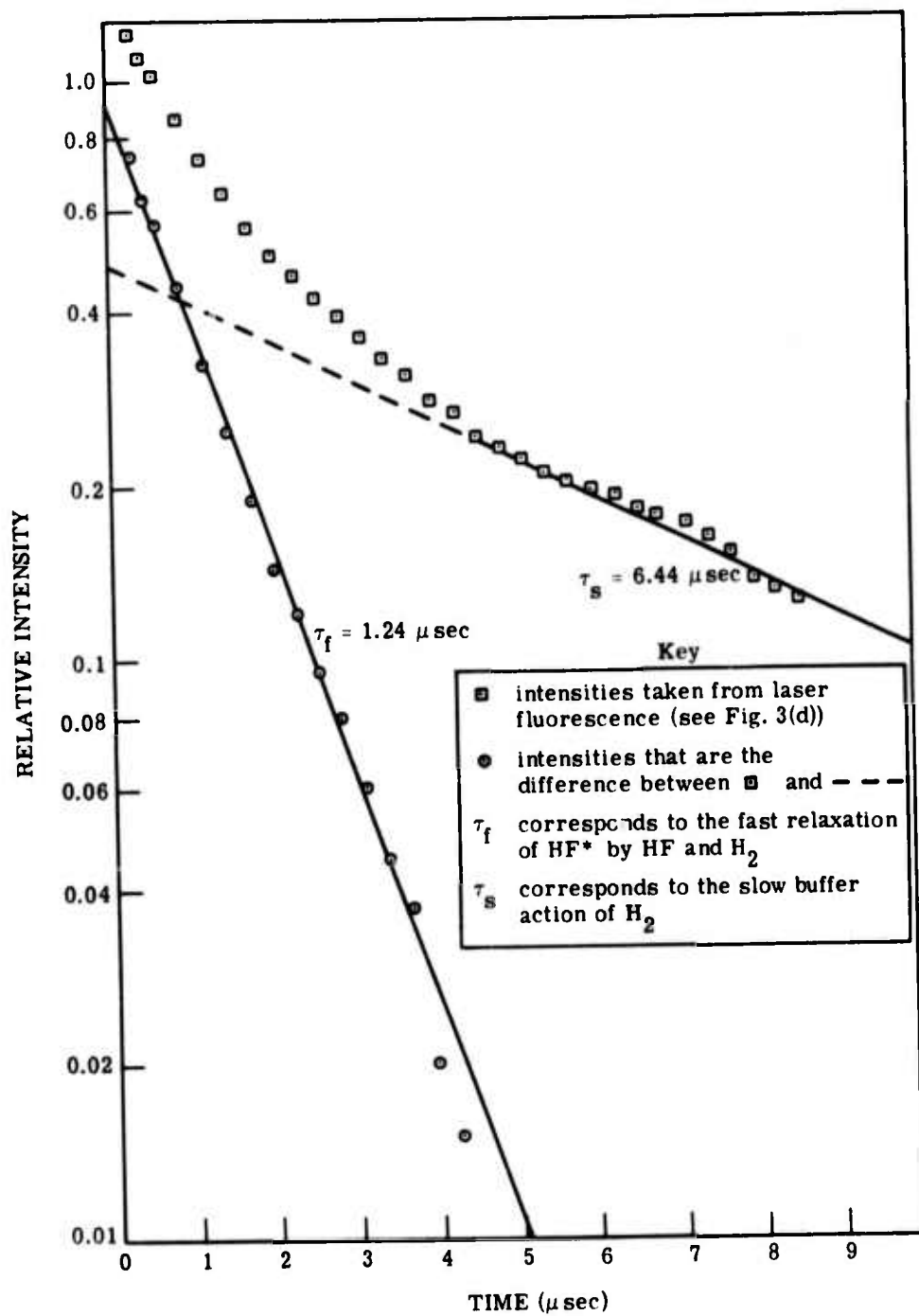


FIGURE 14. HF LASER-DISCHARGE FLUORESCENCE. $\text{H}_2:\text{SF}_6 = 5:20$ Torr.

nsec of the laser pulse was passed unattenuated by the Pockel's cell and the intense infrared radiation excited a single $P_1(J)$ transition of the HF gas into saturation. The laser pulse was then abruptly terminated by optical switching using the Pockel's cell. The intensity of the radiation which 'leaked' through the crossed polarizer of the optical switch was more than two orders of magnitude weaker than that of the pumping radiation and served to probe the excited HF gas.

For the relaxation measurement to be an accurate determination of the rotational relaxation time, the criterion of spectral coincidence between pump and probe must be satisfied as discussed above (Section 3.1). One must be careful here even in the case of a single-pulse technique. Frequency 'chirping,' wherein the frequency of the laser radiation changes with time during a single pulse, would produce erroneous relaxation results* since the pump (leading portion of the pulse) would have a different frequency from the probe (trailing portion). Heterodyne beating between two of our HF lasers produced a uniform, single frequency beat-note indicating spectral purity of our laser [12, 13].

Figure 15 shows how the probe radiation, in the presence of the pumping radiation, goes from a condition of low transmission to one of almost complete transmission as the cell is bleached. When the pumping ceases, the transmission of the gas decreases exponentially as the nonequilibrium condition equilibrates within the vibrational level. This rapid relaxation is due to long range dipole-dipole collisions involving changes in the magnitude of the rotational angular momentum. The time constant for rotational relaxation is plotted in Figure 16 as a function of reciprocal pressure for the $P_1(5)$ and $P_1(6)$ transitions. The relationship is linear as expected, with self-relaxation rate constants of $k_{\text{HF-HF}}$ in close agreement with values obtained from collisional linewidth data [27, 28] obtained at high HF pressures. The observed rotational relaxation times increase with increasing J and may provide the reason for the increase in laser pulse duration with J noted in Section 2.3.1.

Table 1 presents relaxation rates obtained from high pressure linewidth data [27, 28] and from our low pressure data. The relaxation time τ was obtained from the high resolution measurements of the collisional linewidth γ_L of HF [27, 28]

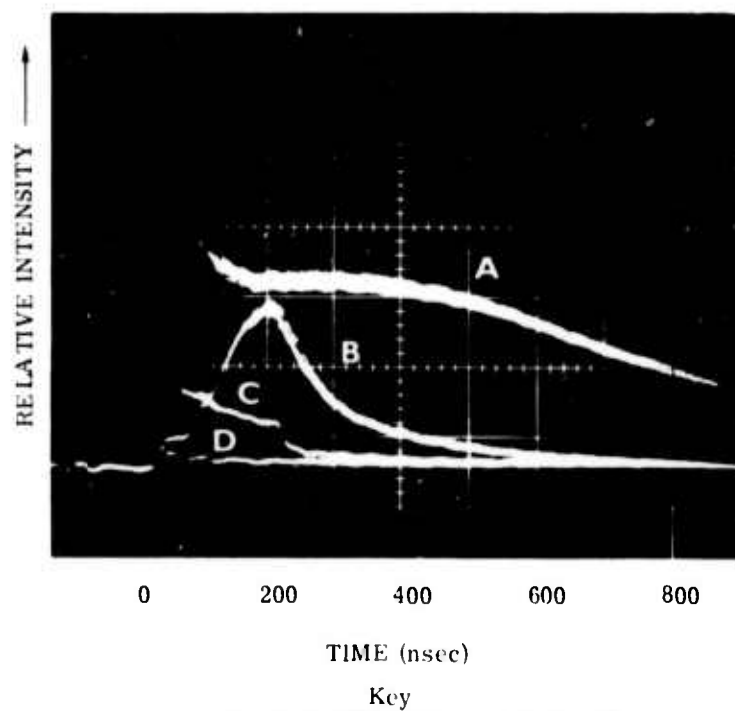
$$\tau = \frac{1}{2\pi c \gamma_L}$$

where c is the velocity of light in vacuum and γ_L is in cm^{-1} .

*A linear 'chirp' would produce a linear rather than exponential relaxation measurement.

27. R. J. Lovell and W. F. Herget, Lorentz Parameters and Vibration-Rotation Interaction Constants for the Fundamental Band of HF, *J. Opt. Soc. Amer.*, **52**, pp. 1374-76 (1962).

28. W. F. Herget, W. E. Deeds, N. M. Gailar, R. J. Lovell, and A. H. Nielson, Infrared Spectrum of HF: Line Positions and Shapes, II, Treatment of Data and Results, *J. Opt. Soc. Amer.*, **52**, pp. 1113-19 (1962).



- Key
- (A)-Incident Probe Signal
 - (B)-Transmitted Probe Signal
in Presence of Pumping
Radiation
 - (C)-Pumping Radiation
(vertical scale com-
pressed by 10^3)
 - (D)-Transmitted Probe
Signal in Absence of
Pumping Radiation

FIGURE 15. OSCILLOSCOPE TRACES OF ROTATIONAL RELAXATION MEASUREMENTS. Each trace is the superposition of about 20 laser pulses.

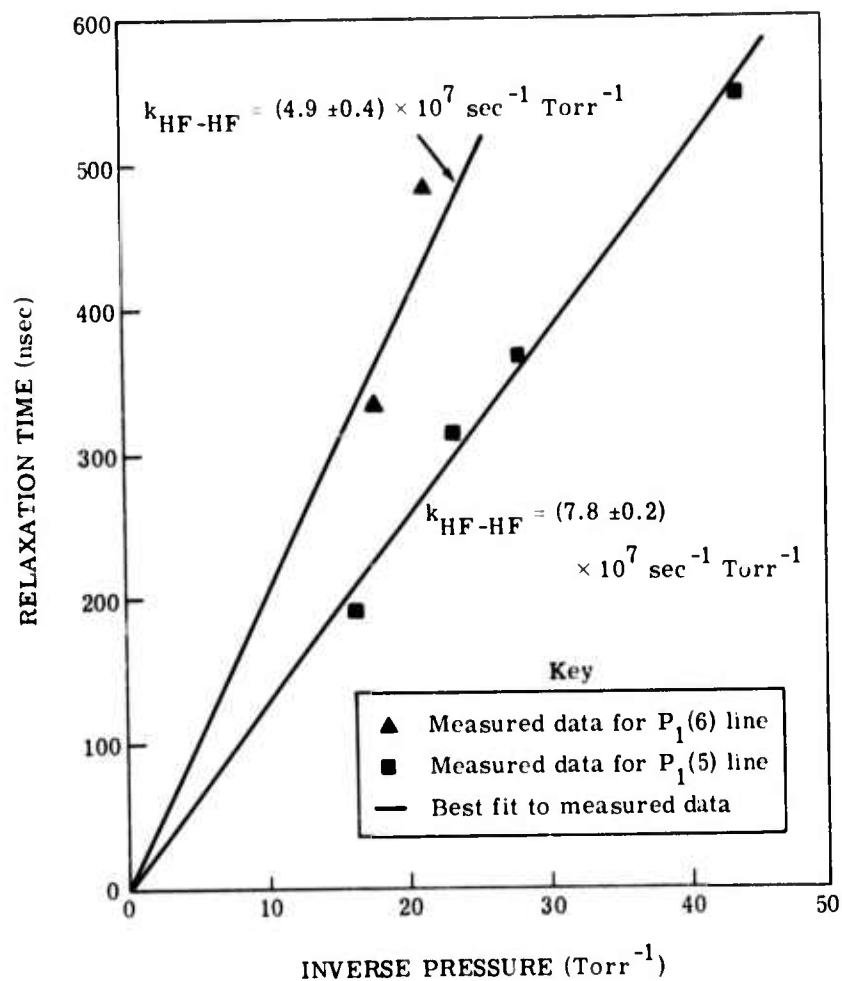


FIGURE 16. RELAXATION TIME AS A FUNCTION OF INVERSE PRESSURE. The self-relaxation rates for the P₁(5) and P₁(6) transitions in HF are shown.

TABLE 1. ROTATIONAL RELAXATION RATES OF HF AT 100°C FROM COLLISIONAL LINEWIDTH DATA^{a,b} AND LASER PUMP-PROBE TECHNIQUE

	Collisional Linewidth Data ^{a,b} ($\tau = 1/2\pi C\gamma_L$)		Laser Pump-Probe Technique (τ measured directly)	
	p (Torr)	$k = 1/\tau p$ ($\text{sec}^{-1} \text{Torr}^{-1}$)	p (Torr)	$k = 1/\tau p$ ($\text{sec}^{-1} \text{Torr}^{-1}$)
$P_1(2)$	760	$13.64^a \times 10^7$		
	760	14.01^b		
	50	13.27^b		
$P_1(3)$	760	$13.49^a \times 10^7$		
	760	13.67^b		
	50	13.35^b		
$P_1(4)$	760	$11.61^a \times 10^7$		
	760	11.24^b		
	50	11.95^b		
$P_1(5)$	760	$7.89^a \times 10^7$	0.062	8.56×10^7
	760	7.32^b	0.043	7.38
	500	8.07^b	0.036	7.61
	50	8.44^b	0.023	8.01
$P_1(6)$	760	$4.32^a \times 10^7$	0.047	4.42×10^7
	760	4.32^b	0.056	5.36
	500	5.96^b		
$P_1(7)$	500	$4.83^b \times 10^7$		

^aRef. [27].

^bRef. [28].

Agreement is good between the high pressure data and data at low pressures where the gas behavior is close to that of an ideal gas.

Relaxation time measurements were made for the $P_1(3)$ and $P_1(4)$ lines. Contrary to the results for $P_1(5)$ and $P_1(6)$, the relaxation time was not linear with HF pressure. Because of the high absorption coefficient for the lower J's, a vibration-rotation transition can be saturated only at the lower pressures in our 30-cm gas cell. At low pressures however, collisional relaxation is slow and it is possible that our measured times are a result of molecular transit time out of the laser beam rather than rotational relaxation. If this is the case, a shorter HF gas cell will be required in order to obtain higher pressures and hence shorter relaxation times without excessive absorption of the pumping laser beam. Time did not permit us to do this however.

A principal mode of vibrational relaxation is through collisional coupling to the rotational degrees of freedom (V - R). Excited, low-J, vibrational levels of HF are nearly resonant with lower vibrational levels when the J of the lower level exceeds approximately 13 (see Figure 2). A pump-probe experiment would therefore be very interesting when probing occurred on a high-J transition. Since relaxation measurements were successful only during the late stages of the program, high-J experiments were not attempted. Lasing action for high-J transitions has been observed [2, 18], although we have had little success in obtaining high-J lines using our lasers. It would appear that operation at high voltages, low pressures (therefore slow relaxation), and long discharges (high gain) with a minimum of loss (internal mirrors) is important.

3.3.4 ROTATIONAL RELAXATION OF HF BY H_2

When helium or air was added to the HF in the gas cell, the relaxation time decreased as expected. However pressures in excess of 1 Torr, the limit of our manometer, were required to produce a measurable change in the HF relaxation time. Hydrogen gas was more effective in relaxing the laser-excited HF.

A few hundred mTorr of H_2 were added to a few tens of mTorr of HF in a static, passivated gas cell. Measurements of HF relaxation were made both before and after the addition of the H_2 gas. The relaxation time of the HF due to the presence of H_2 alone was determined according to the relationship

$$\frac{1}{\tau_{HF-H_2}} = \frac{1}{\tau_{Total}} - \frac{1}{\tau_{HF-HF}}$$

The relaxation due to the presence of H_2 was clearly exponential with a minimum of error. However, agreement between different experimental runs was poor. The relaxation rate of HF in the presence of H_2 gas was measured to be $k_{HF-H_2} = (0.8 \pm 0.3) \times 10^7 \text{ sec}^{-1} \text{ Torr}^{-1} (H_2)$.

It should be noted that this is a preliminary relaxation rate. It does however show that the pump-probe technique can be used to determine the relaxation time of HF with diluent gases, and

more work is necessary toward optimizing the experimental parameters (in particular the choice of HF and additive gas pressures) to reduce the experimental error.

It should also be noted that the presence of H_2 additive gas seemed to eliminate nonlinear optical resonance phenomena such as optical nutations and self-induced transparency (see Section 4) which have complicated our experimental measurements in pure HF gas throughout the investigation. Quite possibly the idea of obtaining relaxation parameters from a computer fit to the time evolution of the saturated absorption may be used in the case of diluent gases. As discussed previously (Semi-Annual Report [12]), nonlinear optical processes prevented us from obtaining rates in pure HF, but the fact that these processes are rapidly damped in the presence of diluent gases lends attraction to using the technique in diluent relaxation measurements.

4

RESONANCE PHENOMENA

4.1 INTRODUCTION

The main purpose of this research work was to measure the relaxation rates of HF gas using time-resolved pulsed laser techniques. However, the waveshape of laser pulses transmitted by HF were found to differ considerably from what would be expected under conditions of usual absorption and saturation [11]. These effects have been attributed to the nonlinear optical phenomena of self-induced transparency [14] and optical nutations [15]. In addition, we have observed laser radiation propagation velocities through HF of as little as 1/40 the velocity of light in vacuum.

4.2 SELF-INDUCED TRANSPARENCY AND OPTICAL NUTATIONS

Self-induced transparency (SIT), first observed by McCall and Hahn [14], is a nonlinear optical transmission phenomenon whereby radiation absorbed in the leading portion of a laser pulse is re-emitted later in the pulse. Two conditions must be met in order to observe SIT: (1) The energy density of the radiation pulse must exceed a threshold value and (2) the pulse duration must be less than the inverse of the homogeneous broadening contribution to the total optical linewidth [14].

For a degenerate gas [15, 29], the first condition is satisfied when

$$\left[\frac{|m|}{6} \left(\frac{1}{2J' + 1} + \frac{1}{2J + 1} \right) \right]^{1/2} \frac{p}{h} \int_0^\infty E(t) dt = 2\pi$$

29. A. Zembrod and T. Gruhl, Self-Induced Transparency of Degenerate Transitions with Thermally Equilibrated Levels, *Phys. Rev. Letters*, 27, pp. 287-89 (1971).

where J' and J are the angular momentum quantum numbers of the upper and lower states of the transition

p is the dipole moment matrix element for the transition [26, 27]

$E(t)$ is the electric field of the laser pulse

$M = J$ for P-transitions and $J + 1$ for R-branch transitions [26]

For P-branch transitions where $J' = J - 1$, this reduces to

$$\left[\frac{1}{6} \left(\frac{4J^2}{4J^2 - 1} \right) \right]^{1/2} \frac{p}{h} \int_0^\infty E(t) dt = 2\pi$$

The second condition is satisfied when the pulse duration is less than the collisional dephasing time of the gas. For HF, the dephasing time τ was shown to be $\tau p \left(= k_{\text{HF-HF}}^{-1} \right) \approx 10^{-8} \text{ sec} \cdot \text{Torr}$ (see Section 3.3.3). For a 100 nsec pulse, the condition is satisfied for HF gas pressures below 100 mTorr.

The Semi-Annual Report [12] presented our observations of SIT in HF gas. Laser pulses were observed whose intensity of radiation transmitted by the HF gas actually exceeded the incident intensity and the net absorption of energy was anomalously small. The threshold laser intensity was found to be in agreement with theory.

For laser intensities in excess of the threshold for SIT, a modulation in the intensity of the transmitted radiation was observed [12]. The oscillations are similar to optical nutation predicted by Tang and Statz [30] and observed by Brewer and Shoemaker [15]. The oscillation frequency Ω was in agreement with that calculated from theory within a few percent

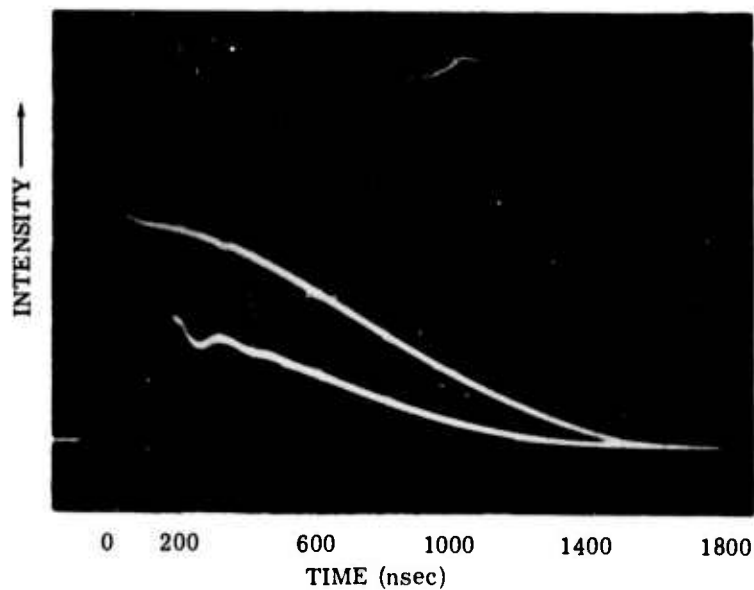
$$\Omega = \left[\frac{m}{6} \left(\frac{1}{2J' + 1} + \frac{1}{2J + 1} \right) \right]^{1/2} \frac{p |E|}{h}$$

Since Ω is linear with applied laser E-field, it should be linear with the square root of the laser intensity. Figure 17 is a plot of the measured optical nutation frequency as a function of normalized intensity. The oscillation frequency, Ω , clearly depends upon the laser intensity or E-field, but the question of its linearity still remains. HF pressure has a pronounced effect on the optical nutation frequency for a given laser intensity. A higher pressure produces a smaller Ω —as would be expected when absorption is considered. This must be accounted for to yield an 'effective' intensity or E-field before the question of linearity is resolved.

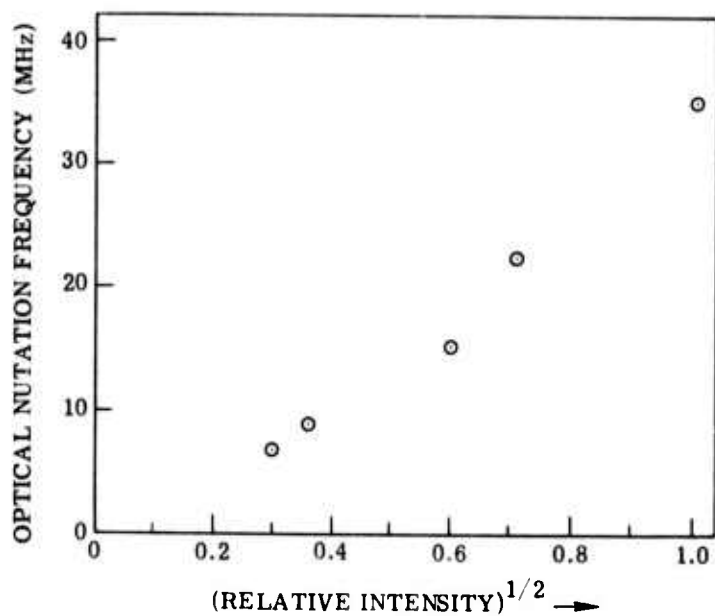
4.3 ANOMALOUS PROPAGATION VELOCITY

While attempting to measure the rotational relaxation time in HF [12], we used the experimental configuration in Figure 18. Usually large time delays were observed for radiation which was propagating in the HF cell when the Pockel cell was switching.

30. C. L. Tang and H. Statz, Optical Analog of the Transient Nutation Effect, Appl. Phys. Letters, 10, pp. 145-47 (1967).



(a) Optical Nutation Trace [12]



(b) Observed Optical Nutation Frequency as a Function of Incident Laser Intensity for the $P_1(5)$ Line. Theory [30] predicts that optical nutation frequency is linear with the applied E-field.

FIGURE 17. OBSERVATIONS OF OPTICAL NUTATION

Figure 18 shows the incident laser pulse (trace A) in the absence of switching and (trace B) with optical switching (i.e., signal at D_2). Traces C and D of Figure 18 show the signal at D_1 . No radiation reaches D_1 before optical switching because the vertically polarized laser light is not reflected by the germanium reflector at Brewster's angle. No radiation reaches D_1 after switching because polarizer P_2 extinguishes the half-wave retarded polarization which exits the Pockel's cell. During switching, however, the Pockel's cell retardation is not half-wave, and vertically polarized radiation passing back through the Pockel's cell will be rotated in polarization such that its horizontal component is reflected by the germanium. The duration of the pulse shown in trace C corresponds to the electrical switching time of the Pockel's cell.

The interesting effect occurred when HF was added to the gas cell. Trace D in Fig. 18 shows this effect. Here, vertically polarized radiation in the gas cell during switching is rotated 90° when it passes through the Pockel's cell. The radiation is now horizontally polarized and is reflected by the germanium to D_1 . Round-trip time through the cell should only be a few nanoseconds and not observable with respect to the longer electrical switching time in trace C. The optical pulse in trace D indicates that the laser radiation is traveling very slowly as it passes through the HF gas — in fact, traveling many times slower than the speed of light in vacuum.

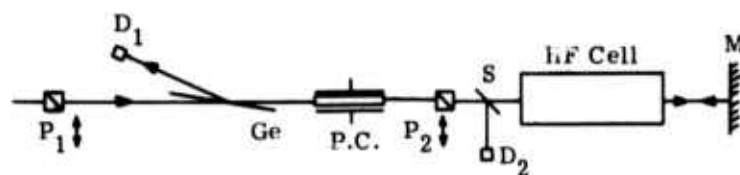
This optical delay increased as the HF gas pressure was increased until a maximum delay was reached. Further pressure increase produced a decrease in delay. Trace D was recorded for $P_1(5)$ laser radiation at a pressure of 37 mTorr of HF where the delay was a maximum. Switching time, trace C, was about 20 nsec and the pulse increased by about 80 nsec in the presence of HF, trace D. This corresponds to a velocity of only 7.5×10^6 m/sec through the 0.60 m path (double-pass) of the gas cell. Or, equivalently, it corresponds to an index of refraction of 40. This optical delay is predicted by the theory for SIT [14] and has been observed in gases [31].

Sizeable pulse delay caused by linear dispersion can occur in any absorbing medium. However, these delays disappear as the medium becomes saturated unless the SIT condition is satisfied [32].

It should be noted that the pulse in trace D is greater than that in C. The vertically polarized radiation found in the gas cell after switching occurs undergoes complete half-wave retardation when it passes back through the Pockel's cell (voltage is on) and is therefore maximally reflected by the germanium.

31. C. K. N. Patel and R. E. Slusher, Self-Induced Transparency in Gases, *Phys. Rev. Letters*, **19**, pp. 1019-22 (1967) and C. K. N. Patel, Investigation of Pulse Delay in Self-Induced Transparency, *Phys. Rev. 1A*, pp. 979-82 (1970).

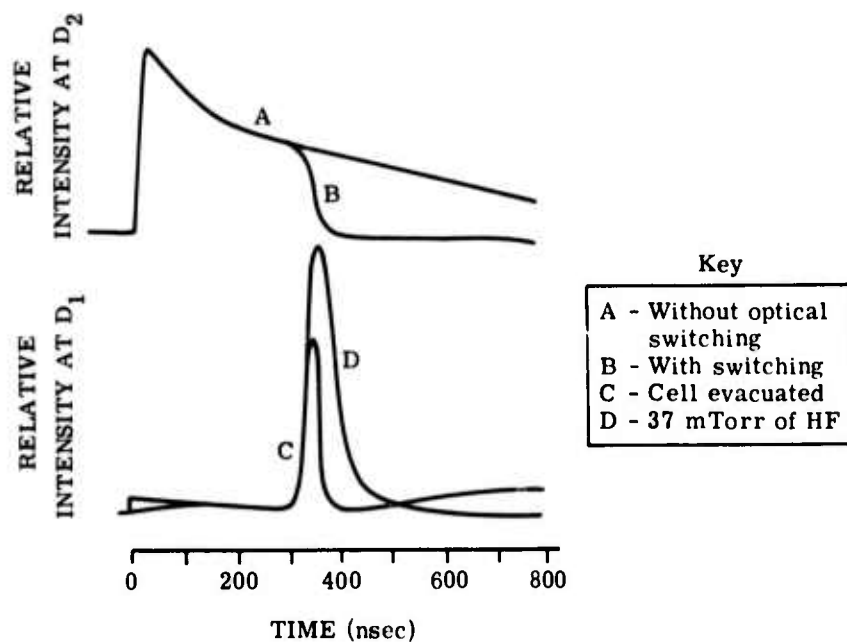
32. C. K. Rhodes, A. Szoke, and A. Javan, The Influence of Level Degeneracy on the Self-Induced Transparency Effect, *Phys. Rev. Letters*, **21**, pp. 1151-55 (1968).



Key

$P_{1,2}$ - Polarizers
 $D_{1,2}$ - Detectors
 Ge - Brewster's angle germanium
 P.C. - Pockel's cell
 S - Beamsplitter
 M - Mirror

(a) Experimental Configuration



Key

A - Without optical switching
 B - With switching
 C - Cell evacuated
 D - 37 mTorr of HF

(b) Observed Traces

FIGURE 18. OBSERVATION OF RADIATION PROPAGATION VELOCITY. The time delay in D corresponds to a propagation velocity in HF which is $1/40$ that in vacuum.

It is also interesting to note that a 100 nsec laser pulse is 10 m long in vacuum yet is only 25cm long in HF gas when $n = 40$. The 10 m pulse can easily be contained in our 30cm gas cell.

It should be noted that the resonant phenomena in this chapter were incidental to our measurements of relaxation rates. We feel that while these effects are extremely interesting, our results are by no means complete. Insight into coherent propagation and resonant processes could be obtained from more extensive studies. Possible applications of SIT include lossless atmospheric propagation and pulse shaping to attain high peak power and short pulse duration for HF laser fusion research (as discussed in the Semi-Annual Report [12]). These interesting physical effects are certainly worthy of further study.

REFERENCES

1. J. V. V. Kasper and G. C. Pimentel, HCl Chemical Laser, *Phys. Rev. Letters*, 14, pp. 352-54 (1965).
2. T. F. Deutsch, Molecular Laser Action in Hydrogen and Deuterium Halides, *Appl. Phys. Letters*, 10, pp. 234-36 (1967).
3. K. L. Kompa and G. C. Pimentel, Hydrofluoric Acid Chemical Laser, *J. Chem. Phys.*, 47, pp. 857-58 (1967) and A. N. Chester and L. D. Hess, Study of the HF Chemical Laser by Pulse-Delay Measurements, *IEEE J. Quant. Electr.*, QE-8, pp. 1-13 (1972), bibliography.
4. C. Wittig, J. C. Hassler, and P. D. Coleman, Continuous Wave Carbon Monoxide Chemical Laser, *J. Chem. Phys.*, 55, pp. 5523-32 (1971).
5. D. J. Spencer, T. A. Jacobs, H. Mirels, and R. W. F. Gross, A Continuous Wave Chemical Laser, *Int. J. Chem. Kinetics*, 1, pp. 493-94 (1969) and T. A. Cool, T. J. Falk, and R. R. Stephens, DF-CO₂ and HF-CO₂ Continuous-Wave Chemical Lasers, *Appl. Phys. Letters*, 15, pp. 318-20 (1969).
6. At the Sandia Laboratory—see, for example, *Electro-Optical Systems Design*, Nov. 1973, p. 6.
7. J. R. Airey and S. F. Fried, Vibration Relaxation of Hydrogen Fluoride, *Chem. Phys. Letters*, 8, pp. 23-26 (1971) and R. R. Stephens and T. A. Cool, Vibrational Energy Transfer and De-excitation in the HF, DF, HF-CO₂ and DF-CO₂ Systems, *J. Chem. Phys.*, 56, pp. 5863-77 (1972).
8. R. M. Osgood, Jr., A. Javan, and P. B. Sackett, Measurement of Vibration-Vibration Energy Transfer Time in HF Gas, *Appl. Phys. Letters*, 20, pp. 469-72 (1972).
9. J. K. Hancock and W. H. Green, Laser Excited Vibrational Relaxation Studies of HF, *J. Chem. Phys.*, 56, pp. 2474-75 (1972).
10. J. F. Bott and N. Cohen, Shock Tube Studies of HF Vibrational Relaxation, *J. Chem. Phys.*, 55, p. 3698 (1971) and J. F. Bott, HF Vibrational Relaxation Measurements Using Combined Shock-Tube, *J. Chem. Phys.*, 57, pp. 96-102 (1972).
11. J. K. Hancock and W. H. Green, Vibrational Deactivation of HF ($v=1$) in Pure HF and in HF-Additive Mixtures, *J. Chem. Phys.*, 57, pp. 4515-29 (1972).
12. L. M. Peterson, G. H. Lindquist, and C. B. Arnold, Rotational Relaxation and Self-Induced Transparency in HF Gas, Report No. 101300-17-P, Environmental Research Institute of Michigan, Ann Arbor, April 1974.
13. L. M. Peterson, C. B. Arnold, and G. H. Lindquist, Pulsed HF Chemical Laser Linewidth Measurements Using Time-Resolved Bleachable Absorption of HF Gas, *Appl. Phys. Letters*, 24, pp. 615-17 (1974).
14. S. L. McCall and E. L. Hahn, Self-Induced Transparency by Pulsed Coherent Light, *Phys. Rev. Letters*, 18, pp. 908-11 (1967) and Self-Induced Transparency, *Phys. Rev.*, 183, pp. 457-85 (1969).
15. G. B. Hocker and C. L. Tang, Observation of the Optical Nutation Effect, *Phys. Rev. Letters*, 21, pp. 591-94 (1968) and R. G. Brewer and R. L. Shoemaker, Photon Echo and Optical Nutation in Molecules, *Phys. Rev. Letters*, 27, pp. 631-34 (1971).

16. G. H. Lindquist et al., Investigations of Chemical Laser Processes, Report No. 191300-1-P, Environmental Research Institute of Michigan, Ann Arbor, February 1973.
17. G. H. Lindquist et al., Investigations of Chemical Laser Processes, Report No. 191300-2-F, Environmental Research Institute of Michigan, Ann Arbor, June 1973.
18. O. R. Wood and T. Y. Chang, Transverse-Discharge Hydrogen Halide Lasers, *Appl. Phys. Letters*, 20, pp. 77-79 (1972).
19. C. R. Jones, Gain and Energy Measurements on an Electrically Pulsed Chemical Laser, *Appl. Phys. Letters*, 22, pp. 653-55 (1973).
20. S. Marcus and R. J. Carbone, Gain and Relaxation Studies in Transversely Excited HF Lasers, *IEEE J. of Quant. Electr.*, QE-8, pp. 651-55 (1972).
21. H. Chen and C. B. Moore, Vibration-Vibration Energy Transfer in Hydrogen Chloride Mixtures, *J. Chem. Phys.*, 54, pp. 4080-84 (1971).
22. F. DeMartini and J. Ducuing, Stimulated Raman Scattering in Hydrogen: A Measurement of the Vibrational Lifetime, *Phys. Rev. Letters*, 17, pp. 117-19 (1966).
23. W. H. Beatie, G. P. Arnold, and R. G. Wenzel, Chemical Efficiency in a Pulsed HF Laser, *Chem. Phys. Letters*, 16, pp. 164-68 (1972).
24. F. J. Zelzenik and R. A. Svehla, Rotational Relaxation in Polar Gases, *J. Chem. Phys.*, 53, pp. 632-46 (1970).
25. P. K. Cheo and R. L. Abrams, Rotational Relaxation Rate of CO₂ Laser Levels, *Appl. Phys. Letters*, 14, pp. 47-49 (1969) and Collisional Relaxation of CO₂ Rotational Levels by N₂ and He, *Appl. Phys. Letters*, 15, pp. 177-78 (1969); R. R. Jacobs, S. J. Thomas, and K. J. Pettipiece, J-Dependence of Rotational Relaxation in the CO₂ 00⁰1 Vibrational Level (to appear in *IEEE J. of Quant. Electr.*, 1974); and T. O. Carroll and S. Marcus, A Direct Measurement of the Rotational Relaxation Time in CO₂, *Phys. Letters*, 27A, pp. 590-91 (1968).
26. R. E. Meredith and F. G. Smith, Investigations of Fundamental Laser Processes, II, Computation of Electric Dipole Matrix Elements for HF and DF, Report No. 84130-39-T(II), Willow Run Laboratories, The University of Michigan, Ann Arbor, November 1971.
27. R. J. Lovell and W. F. Herget, Lorentz Parameters and Vibration-Rotation Interaction Constants for the Fundamental Band of HF, *J. Opt. Soc. Amer.*, 52, pp. 1374-76 (1962).
28. W. F. Herget, W. E. Deeds, N. M. Gailar, R. J. Lovell, and A. H. Nielsen, Infrared Spectrum of HF: Line Positions and Shapes, II, Treatment of Data and Results, *J. Opt. Soc. Amer.*, 52, pp. 1113-19 (1962).
29. A. Zembrod and T. Gruhl, Self-Induced Transparency of Degenerate Transitions with Thermally Equilibrated Levels, *Phys. Rev. Letters*, 27, pp. 287-89 (1971).
30. C. L. Tang and H. Statz, Optical Analog of the Transient Nutation Effect, *Appl. Phys. Letters*, 10, pp. 145-47 (1967).
31. C. K. N. Patel and R. E. Slusher, Self-Induced Transparency in Gases, *Phys. Rev. Letters*, 19, pp. 1019-22 (1967) and C. K. N. Patel, Investigation of Pulse Delay in Self-Induced Transparency, *Phys. Rev.*, 1A, pp. 979-82 (1970).
32. C. K. Rhodes, A. Szoke, and A. Javan, The Influence of Level Degeneracy on the Self-Induced Transparency Effect, *Phys. Rev. Letters*, 21, pp. 1151-55 (1968).

Appendix
THE RELATIONSHIP BETWEEN LASER PULSE SHAPE
AND RELAXATION PROCESSES

The buffer action of H_2 which rapidly relaxes the vibrationally excited HF in the HF laser discharge as discussed in Section 3.3.2 and the rotational relaxation effects observed in Section 3.3.3 lead one to speculate about the nature of the three distinct parts of a single laser pulse as noted in Section 2.3.3 (see Figures 8 and 9).

Consider an HF laser operating on a single vibration-rotation transition and having an electrical pulse which is short compared to the time delay before lasing.

The chemical reaction between the hydrogen and the fluorine atoms generated by the discharge yields vibrationally excited HF. If a total inversion exists between the vibrational levels, lasing will be intense and will likely be depleted rapidly —hence the sharp 'spike' on the leading edge of the laser pulse. Although depletion has destroyed the total inversion, a partial inversion will still exist for most of the P-branch transitions (see Section 2.3). Lasing still occurs (but less intensely) and rotational relaxation between adjacent J-states in the vibrational levels (both upper and lower) prevents the vibration-rotation laser transition from being depleted until the entire vibrational level is depleted —hence the long intermediate region of the laser pulse. Although rotational relaxation maintains the lasing action, vibrational relaxation ($HF - HF$, $V \rightarrow R$, T ; and $HF - H_2$, $V \rightarrow V$) eventually terminates lasing as may be seen by the decrease of laser pulse length and gain as H_2 pressure is increased.

The final portion of the pulse, which gives it the long low intensity tail, may be from the buffer action of the H_2 gas (see Section 3.3.2). The transfer of energy from vibrationally excited HF to H_2 is eventually returned to the HF which may weakly maintain lasing action.